ANALYSIS OF INITIAL CONDENSATION AND THE EFFECTS OF DISTILLERS' SPENT GRAIN PELLET ORIENTATION AND SUPERHEATED STEAM OPERATING PARAMETERS ON EFFECTIVE MOISTURE DIFFUSIVITY

by

JUSTIN BOURASSA

A Thesis submitted to the Faculty of Graduate Studies of

The University of Manitoba

in partial fulfillment of the requirements of the degree of

MASTER OF SCIENCE

Department of Biosystems Engineering

University of Manitoba

Winnipeg, Manitoba

ABSTRACT

Distillers' spent grain (DSG) is a major by-product of ethanol production. DSG has been found to be a good supplement for cattle and swine feed due to its nutrient composition. Lowering the moisture content of DSG by superheated steam (SS) drying has the potential to be a more energy efficient method as compared to hot air drying. A unique phenomenon that exists with SS drying is that condensate will initially increase the moisture content of the sample due to the material temperature being lower than the saturation temperature of the SS.

One objective of this study was to investigate parameters associated with the initial condensation period of SS drying on DSG pellets compacted at a pressure of 60.3 MPa. These parameters included the maximum condensation, condensation time, and restoration time. Two methods were used to investigate the effects of SS temperature (120, 150, and 180 °C) and velocity (1.0, 1.2, and 1.4 m/s) on the condensation period, one based on direct mass measurement and the other based on measured DSG pellet surface temperature. An increase in SS temperature from 120 to 180 °C and SS velocity from 1.0 to 1.4 m/s resulted in a 97% and 67% decrease in maximum condensation, respectively.

Another objective of this study was to determine the effect of SS temperature (120, 150, and 180 °C), velocity (1.0 and 1.2 m/s), and orientation with respect to the direction of SS flow on the effective moisture diffusivity of DSG pellets. The diffusion model used was based on a finite cylinder geometry while accounting for volumetric shrinkage. The diffusivity coefficient of DSG was determined to be 1.56×10^{-8} m^2/s. A significant effect of orientation on effective moisture diffusivity ($P<0.0015$) was found only during the constant drying-rate period.

ACKNOWLEDGEMENTS

I would like to thank Dr. S. Cenkowski for his guidance, support, and funding during my graduate program. I would also like to thank the other members of my committee, Dr. Y. Chen and Dr. H. Soliman.

I would like to thank Matt McDonald, Dale Bourns, and Robert Lavallee for their technical assistance with this study.

I would also like to thank Rani Puthukulangara for her assistance with preparing samples and running experiments.

I gratefully acknowledge the financial support provided by the Natural Sciences and Engineering Research Council of Canada (NSERC).

TABLE OF CONTENTS

LIST OF TABLES

LIST OF FIGURES

1 LITERATURE REVIEW

1.1 Preamble

Distillers' spent grain (DSG) is a major by-product of ethanol production. Spent grains are also the by-products from the production of alcoholic beverages. It has been reported by Bonnerdeaux (2007) that one ton of corn or wheat can be fermented to produce approximately 375 L of ethanol. The DSG that is left behind after fermentation per ton of corn or wheat is approximately 470 kg (Graham et al., 2013). In the US in 2009, the sale of DSG from ethanol plants contributed up to 20% of their total income (Ileleji, 2010). As of 2013 it has been reported that the production of ethanol is projected to increase by approximately 67% over the next ten years (OECD Agricultural Outlook, 2014), leading to an increase in supply of DSG. Some predictions go far enough to indicate that there will be an oversupply of DSG which could affect the future viability of the ethanol industry (Bonnardeaux, 2007). However, it is important to note that these predictions were made when the price of oil was approximately $100 per barrel in 2014 and did not account for the political and economic impacts that reduced the price by nearly 50% near the start of 2015. Taking these factors into account, the updated predictions on the amount of ethanol and DSG production long-term is still to be determined.

1.2 Potential uses for distillers' spent grain

The coarse grain fraction of DSG has been found to be an excellent source of protein and energy (Nyachoti et al., 2005). DSG makes a good supplement for swine and cattle feed due to it containing high amounts of digestible fibre, protein, and fatty acids, as well as a low amount of starch (Cromwell et al., 1993; Ayoade et al., 2014). However, the nutrient

composition of DSG is heavily influenced by the type of grain used, grain quality, extent of fermentation, and drying conditions used (Cenkowski et al., 2012).

Deoxynivalenol (DON) is a contaminant that is commonly found in wheat and corn crops, and consequently is present in DSG. The level of DON contamination varies with location and year. In a study by Pirgozliev et al. (2009) they found untreated wheat samples from 2008 contained an average DON concentration of 11 ppm in Ontario and 4.5 ppm in Quebec. DON is problematic for DSG consumption by swine because higher levels can result in oxidative stress, increasing intestinal permeability, and inhibiting protein synthesis (Wu et al., 2014). In addition to swine and cattle feed, DSG can be used to produce food products for humans such as baked snacks and baby food (Rasco et al., 1990).

1.3 Moisture content of distillers' spent grain

One drawback to the utilisation of DSG for consumption is that it has high initial moisture content after the fermentation process. It has been reported that DSG leaving the distillation column has moisture content in the range of 75 – 85% wb (wet basis) (Tang & Cenkowski, 2001). Long term transportation and storage of DSG without any further processing becomes unfeasible both from an economic and practical point of view. The large mass of water present in DSG makes transportation costs expensive. Additionally, the water causes DSG to spoil within a short time period making it unsuitable for consumption. Lowering the moisture content helps to reduce microbial and enzymatic reactions at the cost of potentially having an adverse effect on chemical, physical and nutritional values of the food product (Pronyk et al.,

2004). To prolong the shelf life of DSG and make it economical for transport, it has been reported that it should first be dried to a moisture content of 10% wb (Woods et al., 1994).

1.4 Processing of distillers' spent grain

In general, the DSG is screened and pressed or centrifuged to obtain the thin stillage and coarse grain fractions (Bonnardeaux, 2007). Thin stillage can then be evaporated to produce thick syrup with high nutritional value or added back to the spent grains while drying to produce coarse grains with solubles (Stroem et al., 2009). Drying the coarse grain fraction of DSG is most commonly done by hot air drying, however it is considerably difficult due to the products stickiness. Stroem et al. (2009) had reported that the quantity of DSG sticking to the inside of a rotary drum dryer decreased with a decrease in initial moisture content. Another drying method that has been utilised for DSG is superheated steam (SS) (Tang, 2010). It has been reported that while drying DSG in SS major nutrient levels, determined calorimetrically, enzymatically, and with combustion nitrogen analysis, were not affected by increasing the processing time or SS temperature in the range of 105 to 175 °C (Cenkowski et al., 2007). In addition to drying, densification of DSG, the process of reducing its volume and moisture content, could further benefit the utilisation of DSG by reducing the cost of transportation, handling, and storage (Johnson et al., 2013). Another drawback of the utilisation of DSG is the possible contamination of toxins from fungal growth including mycotoxins from the *Fusarium* species. However, with the use of SS processing it may be possible to reduce mycotoxins to a level that is low enough for the DSG to be sold for animal feed purposes. In a study by Pronyk et al. (2006) it was found that DON levels were reduced by up to 52% in naturally contaminated

wheat kernels when processed in SS at 185 °C. Significant reductions were also observed for SS processing at 160 °C. Furthermore, no reduction was found when processing at lower SS temperatures (110 and 135 °C) and steam velocity had no effect on the DON level reduced. Current hot air drying techniques are unable to reduce mycotoxins to such an acceptable level of approximately 4 ppm (Cenkowski et al., 2007; Wu et al., 2014).

1.5 Drying with superheated steam

SS is generated when the temperature of saturated steam is increased under constant pressure. SS can also be generated by reducing the pressure of saturated steam. SS works as a drying medium by evaporating water from food products based on a temperature difference between the SS and the saturation temperature of the wet product (Head et al., 2010). Therefore, SS has the ability to absorb moisture as long as the temperature of the SS stays above the saturation point (Head et al., 2011).

At the start of SS drying evaporation occurs on the external surfaces of the material, and while these surfaces remain wet the evaporation temperature remains at the saturation temperature; therefore the drying rate only depends on the convective heat transfer rate from the SS (Elustondo et al., 2002). The convective heat transfer rate during this constant drying-rate period is highly dependent on the SS temperature and its velocity, with an increase in either parameter resulting in an increased drying rate. However, the coefficient of mass transfer will only increase with an increase in SS velocity up to a certain saturation value (Shibata & Mujumdar, 1994). Increasing the SS velocity beyond the saturation value will not result in an improvement in mass transfer (Urbaniec & Malczewski, 1997). During the falling

drying-rate period the saturation value of the mass transfer coefficient decreases and can be attained at lower SS velocities. The moisture that exists in a wet product can be in many forms including but not limited to free moisture, capillary moisture, colloidal moisture, and chemically attached moisture (Potter & Beeby, 1994). There is a pressure that is exerted between this moisture and the material. With the moisture inside the material exerting lower pressure than the operating SS pressure on the material the moisture is much harder to remove since it is more strongly bound to the material. The material will continue to lose moisture in a combination of forms such as free moisture and capillary moisture until the drying medium pressure is equivalent to the pressure the moisture inside the material is exerting on the material (Pronyk et al., 2010). Therefore, one big consideration in the operating conditions of using SS as a drying medium is the operating pressure. Using higher pressure results in an increased water equilibrium temperature and reduces the heat transfer driving force (Elustondo et al., 2002). On the other hand, using lower pressures reduces the SS density and decreases its heat transfer capacity. In comparison to hot air drying, a decrease in operating pressure results in a smaller difference between drying times of SS and hot air (Tatemoto et al., 2005).

One of the most important aspects of drying studies is to create mathematical models that accurately reflect the drying process. However, in order to produce such models the drying kinetics of the material to be dried must first be determined (Pronyk et al., 2004). Previously equations have been proposed by Tang & Cenkowski (2001) in order to relate the equilibrium moisture content (EMC) to SS conditions. The first equation relates EMC (M_e) to the SS temperature (T):

$$M_e = k\exp[a(T-100)^b] \quad (1.1)$$

The second equation relates EMC to the relative pressure (P_r):

$$M_e = k\exp(aP_r{}^b) \quad (1.2)$$

Where *k*, *a*, and *b* are all coefficients.

These equations were used in the study mentioned and were found to accurately describe the EMC values of spent grain dried in SS at temperatures between 105 and 180 °C.

In general the entire SS drying process can be summarized into four stages: initial condensation, restoration, constant drying-rate, and falling drying-rate periods.

1.5.1 Initial condensation period and restoration period

The initial condensation period, which is unique to SS drying, occurs when a material at a temperature lower than the saturation temperature is exposed to SS. This stage is very important for the modeling of SS drying characteristics as it affects drying kinetics (Taechapairoj et al., 2003). The SS coming in contact with the material becomes cooled and condenses on the material surface as sensible heat is transferred to the material. This results in an overall increase in mass of the sample resulting in increased moisture content. This phenomenon can have a significant effect on the material quality after drying due to quicker heating of the interior of the material (Iyota et al., 2001). Depending on the porosity of the material the condensed moisture has the ability to permeate into the interior of the material. A study by Iyota et al. (2001) reported that the moisture content slightly inside the surface of potato samples had higher moisture content than the original value shortly after the start of SS drying.

Once the material surface temperature increases to the saturation temperature the condensation period is over and the restoration period begins. During the restoration period the remaining condensation evaporates and the moisture content of the material returns to its original moisture content.

1.5.2 Constant drying-rate period

Once the restoration period has finished the process then enters the constant drying-rate period. Here, the sample temperature is supposed to be kept constant at the boiling point while the rate of drying remains constant (Sano et al., 2005). The drying rate has a maximum value that can be attained under the operating pressure and will generally increase with an increase in either SS temperature or velocity. This period generally sees the removal of any remaining free moisture which holds a higher pressure against the material being dried in comparison to the operating pressure of the SS. A previous study done on SS drying of spent grains by Pronyk et al. (2004) has found that the constant drying-rate period did not exist, even with an initial moisture content of approximately 80% wb.

1.5.3 Falling drying-rate period

The falling drying-rate period follows the constant drying-rate period. Now the drying rate begins to decrease as the moisture content of the material is further reduced. The moisture being removed in this stage is primarily the capillary and physically absorbed moisture that is exerting lower pressure on the material being dried. The drying rate can no longer be increased by increasing the SS velocity but rather the SS velocity can be decreased and still maintain the optimum drying rate during this period given that the mass transfer coefficient is

kept above the saturation value. The only way to increase the drying rate at this point would be to increase the operating pressure of the system (this would cause the process to go back into a constant drying-rate period before starting another falling drying-rate period at lower moisture content).

1.6 Comparison of superheated steam drying to hot air drying

In an SS environment, the operating pressure is equal to the partial vapour pressure since the drying medium is composed only of water vapour (Pronyk et al., 2010). Therefore, it has been suggested by Shibata et al. (1990) that in general using SS as a drying medium is superior to hot air drying in reduced pressure operations. This may not be entirely true if only overall drying times are looked at. During the constant drying-rate period of both SS and hot air drying there exists an inversion temperature at which point SS and hot air drying rates are identical (Nomura & Hyodo, 1985). Drying in SS at a temperature higher than the inversion temperature results in an increased drying rate during the constant drying-rate period when compared to hot air drying. Therefore it may be argued that using SS as a drying medium is only superior to hot air drying when the drying temperature is above the inversion temperature. However, it has also been reported that drying in the falling drying-rate period could be quicker in SS over hot air drying under certain operating conditions (Hyodo & Yoshida, 1976). Aside from drying rates it is also important to discuss the other advantages that SS drying has over hot air drying in order to determine which method is more beneficial in certain applications.

In general the benefits of SS drying have been reported to include lower overall energy consumption, elimination of risk for fire and explosions, and the elimination of harmful

emissions (Pronyk et al., 2010). The elimination for risk of fire occurs because the replacement of hot air with SS eliminates air from the drying medium surrounding the processed product, which also reduces the potential for oxidation (Head et al., 2011). Furthermore, it has been suggested by Pronyk et al. (2008) that the future of utilizing SS may not always be in the form of strictly drying, but also product processing. As a processing medium, SS has the ability to change the properties of a product in ways that would not be possible with hot air drying. Devahastin & Suvarnakuta (2004) has reported that in biological materials properties that have the potential to be affected by SS processing include starch gelatinization, enzyme destruction, protein denaturation, color changes, texture changes, and deodorization. In addition, the overall taste of a product can be affected by SS processing since the steam strips more of the acids that contribute to undesirable tastes and aromas (Mujumdar, 2000). Physical changes have also been reported, as in the case of pork drying by Moreira (2001) where the dried product had a higher porosity and lower degree of shrinkage compared to hot air drying at the same temperature.

At first glance from an energy point of view hot air drying looks to be the better choice over SS drying. However, SS drying can be performed in a closed loop system as long as the pressure inside the system is kept constant. The only energy input would be the addition of sensible heat to keep the SS in the superheated state. Therefore, most of the energy associated with evaporating moisture can be recovered by condensing the purged SS and a high energy input is not required to heat the recycled SS from ambient temperature conditions (Fitzpatrick, 1998).

Drying with SS is not without its own set of disadvantages. The main disadvantage of SS drying is that it has the ability to cause damage to heat sensitive materials since the product temperature has to generally remain above 100 °C if dried under atmospheric conditions over the course of drying (Li et al., 1999). Since the drying steam is in direct contact with the product, the product temperature rapidly rises to 100 °C under atmospheric pressure. Again, this problem can be alleviated somewhat by operating at a reduced pressure. Therefore, for thermolabile products the quality of the dried product is the main influence in the selection of operating pressure when drying in SS (Elustondo et al., 2002). Another limitation of SS drying is the complexity of the drying system. The overall size of a SS system may be smaller in comparison to a hot air drying system, however the number of components required to generate SS may outweigh hot air drying from an economic and simplistic point of view (DiBella, 1996).

1.7 Diffusivity background

Diffusion can most generally be described as any transport associated with random motions (Socolofsky & Jirka, 2005). Another property of diffusion is that transport (either of mass or energy) occurs from regions of high concentration to low concentration until an equilibrium state is reached. When describing diffusion as a property of a material a common practice is to use a constant called the diffusivity coefficient. However, in some cases with biological materials the diffusivity coefficient is not suitable to describe the drying kinetics. If the boundary condition of the first kind is acceptable, meaning that temperature of the material is a function of both position and drying time, then it has been reported that diffusivity

should increase when the moisture content of the material is decreased (Silva et al., 2008). In other words the diffusion coefficient can be highly dependent on temperature and concentration. For materials that are heterogeneous the diffusion coefficient can also depend on mass transfer direction, and its value can vary along the diffusion path (Efremov et al., 2008).

1.8 Determination of moisture diffusivity

The determination of moisture diffusivity within a food material over the course of drying can be a complex task since it can exist in many forms such as molecular diffusion, liquid diffusion, vapour diffusion, hydrodynamic flow, capillary flow, Knudsen flow, and surface diffusion (Karathanos et al., 1990; Hashemi et al. 2009; Kim & Bhowmilk, 1995). Furthermore each component can be broken down into a product of other factors. Looking at molecular diffusion for example, diffusivity depends on the phase, temperature and molecule size (Socolofsky & Jirka, 2005). Specifically for granular material it has been widely accepted that the majority of moisture loss is comprised of liquid and vapour diffusion. Therefore, the term "effective diffusivity" is used to describe all possible mechanisms of moisture movement within a biological material. For drying applications, replacing the diffusion coefficient with effective diffusivity helps to alleviate the problem of unsteady moisture diffusion (Maroulis et al., 2001). Knowing the effective moisture diffusivity of a material is necessary for designing and modeling mass transfer processes such as dehydration, adsorption, and desorption of moisture during storage (Erdogdo & Turhan, 2006). Fick's law of diffusion incorporated into drying experiments

has been widely used to determine effective moisture diffusivity for many biological materials (Da Silva et al., 2008; Bourassa et al., 2015).

1.9 Finite and infinite geometry assumptions

Equations have been derived for use to determine effective moisture diffusivity for a wide variety of geometrical shapes. Selecting an equation imposes certain assumptions on the model. For a cylinder, equations exist for both finite and infinite applications. The criteria for choosing one or the other is somewhat left to personal preference. In the study done by Silva et al. (2008), an infinite cylinder model is suggested for use when the radius of the product is much smaller than its length. For rough rice, that model was chosen with the justification that the radius of rice grains was significantly smaller than its length, with a ratio of approximately 1:7 (Hacihafizoglu et al., 2008). Similarly, for the drying of pomegranate arils, the infinite cylinder model was chosen assuming that mass transfer was symmetric to the center of the cylinder with no significant effects of diffusion being contributed from the ends of the cylinder (Erdogdo & Turhan, 2006). It has been suggested by Incropera & DeWitt (1996) that an infinite cylinder model could be used accurately if the length of the sample is at least ten times larger than its radius. However, in a study done by Rovedo & Viollaz (2000) it has been suggested that even with the length being twenty times larger than its radius the model can be inaccurate and the finite model should be used. Therefore, the same material can be analyzed with different geometrical models. A good example of this is the drying and effective diffusivity determination of bananas. In one study done by Thuwapanichayanan et al. (2011) the banana slice was assumed to have the shape of an infinite slab since the thickness was approximately 3 mm. In

another study done by Da Silva et al. (2013) the banana slices were represented by a finite cylinder model since the thickness was closer to 21 mm. Furthermore, a comparison was made in that study which showed that the infinite cylinder model was a poor choice to simulate the drying kinetics over the finite cylinder model.

1.10 Volumetric Shrinkage

Another factor to consider when determining effective diffusivity is how to account for volumetric shrinkage of the material. Volumetric shrinkage in biological materials has been found to be a function of moisture content (Souraki & Mowla, 2007). Decreases in dimensions are caused by heating and loss of moisture which causes stress in the cellular structure of the food product (Mayor & Sereno, 2004). In a study done by Erdogdo & Turhan (2006), the volumetric shrinkage of litchi flesh was assumed to be equal to the volume of water that was being evaporated. The simultaneous assumption in their study was that the pore space in the product was always occupied by moisture in the liquid phase. For the effective diffusivity determination of DSG dried in SS a comparison was done between accounting and not accounting for volumetric shrinkage with the outcome being that shrinkage had a significant effect on the effective moisture diffusivity, especially with increased drying temperatures (Zielinska & Cenkowski, 2012). These results are further supported by Mulet (1994) who showed that volumetric shrinkage of wet biological materials significantly influences moisture diffusivity and advises that volumetric shrinkage should always be taken into account.

2 RESEARCH OBJECTIVES

There are three objectives that were explored in this study:

1. To model the amount of condensation on DSG pellets dried with SS based on their measured surface temperature and compare the predictions to the measured values of condensation.
2. To determine the effect of DSG pellet orientation with respect to the direction of SS flow on effective moisture diffusivity when drying in SS at 120 °C.
3. To determine the effective moisture diffusivity of DSG pellets dried in SS taking into consideration volumetric shrinkage and the effect of SS temperature and its velocity.

3 MATERIALS AND METHODS

3.1 Superheated steam processing system

The SS processing system used for initial condensation and diffusivity experiments was designed and fabricated at the Department of Biosystems Engineering, University of Manitoba (Tang, 2010). A process flow diagram of the SS system can be seen in Fig. 3.1. The system consists of a water reservoir (1) that supplies water by a centrifugal pump (3) to a boiler (8). The boiler produces saturated steam at approximately 0.59 MPa which is then sent through a pressure reducing valve (12). The pressure reducing valve reduces the pressure of the saturated steam to near atmospheric pressure resulting in SS. The temperature of the SS is then increased by the superheater (14) which is controlled by the main electrical panel. The SS leaving the superheater either goes into the drying chamber (20) or back to the water reservoir depending on the position of the 3 way manual valve (19). The steam flow rate is controlled by a globe valve (9) and monitored by a pressure gauge (13). The drying chamber is surrounded by 20 strip heaters that provide heat to the outside walls of the chamber to prevent heat loss from within the drying chamber. SS leaving the drying chamber passes through a heat exchanger (23) where it condenses and can be recycled back to the main water reservoir or diverted through an open tube (24) to collect the condensate which can be used for calculating the SS velocity. A cross sectional schematic of the SS drying chamber showing the location of the fan and electronic balance is shown in Fig. 3.2.

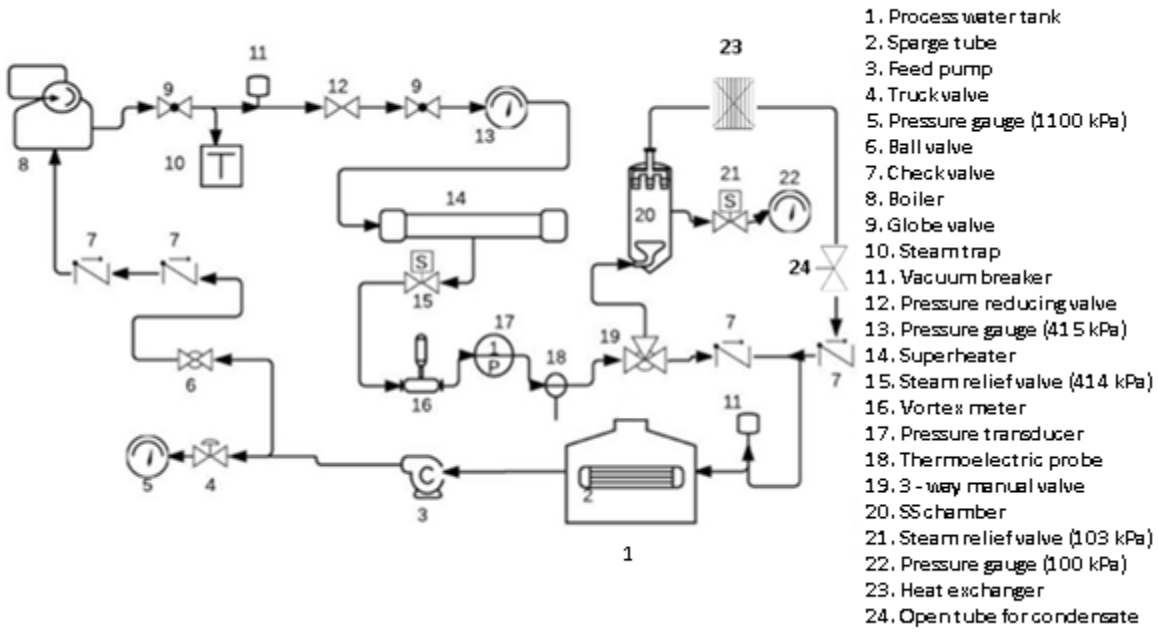

Figure 3.1. Process flow diagram of superheated steam system (Modified from Barychyn D., 2015)

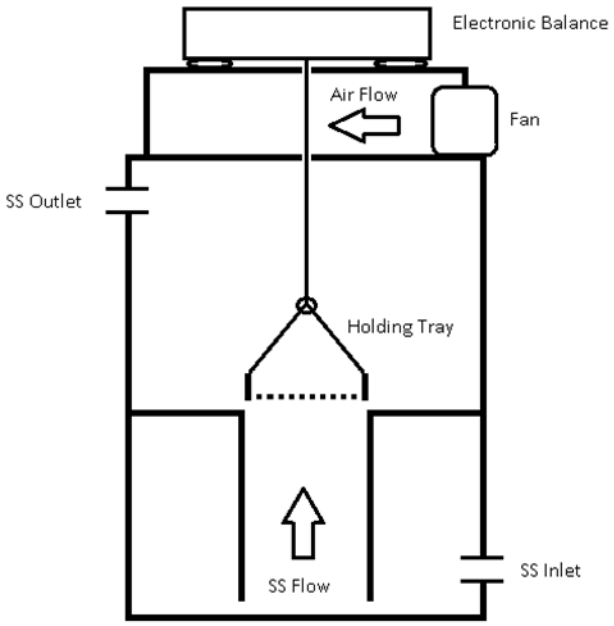

Figure 3.2. Cross section of the SS drying chamber showing the location of the holding tray and location of electronic balance

3.1.1 Modifications to existing superheated steam system

In 2014-15 two modifications were made to the SS processing system which affected the way the system operated. The first modification was adding the ability to remove the 3-way solenoid valve (19, Fig. 3.1.), which directed the SS to either the water reservoir or the drying chamber, and use a 3-way manual valve in its place. The benefit using of the 3-way manual valve is that it reduces the amount of time that it takes for the valve to switch from the water reservoir to the drying chamber. Reducing the transition time reduces the amount of time that the sample is subjected to a highly variable SS flow rate from approximately 30 s with the solenoid valve to 8 s with the manual valve which became very important during the initial condensation experiments. The drawback to using the manual valve is the magnitude of the variable SS flow rate became much higher during the 8 s transition time.

The second modification to the SS system was the addition of approximately 4.5 m of pipe insulation to areas that previously had no insulation. Additionally, a 100 mm thick layer of insulation was added to the outside of the drying chamber to further prevent heat loss. One benefit of increasing the amount of insulation is increased safety due to there being less high temperature areas directly exposed that could be accidentally touched. The other benefit to increasing the amount of insulation is reducing the amount of energy loss within the system. The operating laboratory manual for the SS system has tabulated values to be used on the main electrical panel (which controls the temperature of the superheater) to account for heat loss within the system. With the addition of insulation those values are no longer accurate and a new set of values had to be determined experimentally. Table 3.1 shows the panel temperature

settings suggested by the operating laboratory manual (Gervais, 2008) and Table 3.2 shows the new suggested values determined experimentally. The tables indicate temperatures in °F and °C as the manufacturer provided a display on the main electrical panel that only operates in °F.

Table 3.1. Main electrical panel temperatures for various desired SS chamber temperatures and velocities from original user's manual

Desired SS Chamber Temperature (°C)	Desired SS Velocity (m/s)		
	0.5	1	1.5
120	490°F/254°C	360°F/182°C	290°F/143°C
150	585°F/307°C	440°F/227°C	395°F/201°C
180	N/A	N/A	N/A

Table 3.2. Main electrical panel temperatures for various desired SS chamber temperatures and velocities determined experimentally after modifications

Desired SS Chamber Temperature (°C)	Desired SS Velocity (m/s)		
	0.5	1	1.5
120	335°F/168°C	320°F/160°C	300°F/149°C
150	420°F/216°C	380°F/195°C	375°F/191°C
180	580°F/304°C	N/A	N/A

3.1.2. Determination of superheated steam velocity

After the SS has been condensed by the heat exchanger the water can be diverted out of the system to an open tube (24, Fig. 3.1). The open tube is placed above a volumetric beaker and the time (t_C) is recorded for the water level in the beaker to reach 300 mL. The specific volume, $\upsilon(P_C, T_{SS})$ of the SS is found from tabulated values (Khurm, 2005) being a function of the drying chamber gauge pressure (P_C) and SS temperature (T_{SS}). The SS temperature was measured by a thermocouple which was located inside the SS drying chamber at approximately the same height as the holding tray. The drying chamber pressure was taken from a pressure gauge attached to the SS drying (22, Fig. 3.1) chamber and ranged from 0.1 – 0.3 psi (0.7 – 2.1 kPa) depending on the SS flow rate. The condensate collected had a temperature of approximately 10 °C, therefore the density of water is very close to 1000 kg/m^3 and the mass of

the condensate collected will be 300 g. The velocity (**v**) of the SS going through the drying chamber right below the sample holding tray can then be calculated using the following equation:

$$\mathbf{v} = \frac{0.3v}{t_c A_C} \qquad (3.1)$$

Where A_C is equal to 6.32×10^{-3} m^2 and is the cross sectional area of the inlet pipe to the drying chamber right below where the sample holding tray is located. The error associated with calculated values using Eqn. 3.1 is 0.02%.

3.1.3 Fabrication of heavy sample holding tray and improvements to mass measurement

A light holding tray that has been used for drying experiments that required mass recording can be seen in Fig. 3.3 (Johnson et al., 2014; Zielinska & Cenkowski, 2012). It is comprised of plastic mesh (1 mm) and an aluminum foil ring (diameter of 60 mm) with 4 thin wires attached to the sides that join up to create a hook. The hook is attached to a thin wire of the same material inside the drying chamber that is attached to the underfloor weighing hook of an electronic balance (Model TR-403, Denver Instrument Co., Arvada, CO, USA) located on top of the SS drying chamber. The major drawbacks of this design were found to be that the hook on the light tray was not always directly above the center of the tray, it had a small capacity to hold samples, and it was not rigid. Furthermore, the thin wire attached to the electronic balance was not straight and could touch the inside of the holes that it went through between the electronic balance and the drying chamber. While running experiments, the light holding tray would move around inside the drying chamber due to its small mass (1.9 g). Main causes for the movement of the light tray included the variable SS flow rate (approximately

20%) and the presence of a fan on top of the drying chamber (see Fig 3.2) that was used to prevent SS from reaching the electronic balance but was also blowing air directly onto the thin wire that the light tray was hanging from.

Figure 3.3. Light sample holding tray with 4.2 g DSG pellet for reference

The new design (heavy tray) that was fabricated and used for the experiments in this study can be seen in Fig. 3.4. It was made of an aluminum ring with an outside diameter of 88 mm, thickness of 5 mm, and height of 14 mm. Steel mesh (1 mm) was used for the bottom of the heavy tray with steel pins inserted to hold samples in place. Three thin steel rods were attached to the top of the ring equidistant apart and joined together at the top by a steel loop. The top loop was then attached to a thin steel rod (3.2 mm diameter) which was attached to the underfloor weighing hook of an electronic balance (PGW 453e, Adam Equipment Inc., Danbury, CT, USA) located on top of the SS drying chamber. The loop on top of the tray acted to make sure that the point of attachment to the thin steel rod was very close to being directly over the center of the heavy holding tray. The thin steel rod was rigid enough that it was not affected by the fan used to divert SS away from the electronic balance. The total mass of the

heavy tray and thin steel rod was approximately 124 g, therefore the SS did not cause the holding tray to move significantly while running experiments. The one drawback of using this design was that the overall increase in mass creates a larger ratio of tray mass to sample mass.

Figure 3.4. Heavy sample holding tray with 2.1 g (top) and 4.2 g pellet (bottom) for reference

Another change that was implicated to improve mass measurement was the addition of a glass box on top of the electronic balance to prevent any fluctuations due to air movement. The electronic balance measures mass that is placed on top (conventional weighing) in addition to mass hanging below (underfloor weighing). The addition of the glass box isolated the conventional weighing feature and any mass changes were assumed to be caused by a flux in mass present only attached to the underfloor weighing hook.

Two calibration weights (Troemner Precision Weights, Thorofare, NJ) were used to calibrate both the electronic balance used to measure samples before and after SS drying (Adventurer Pro AV313, Ohaus Corporation, Pine Brook, NJ) and the electronic balance located on top of the SS drying chamber (PGW 453e, Adam Equipment Inc., Danbury, CT, USA) to record

mass changes while drying. The 100 g weight was used to calibrate the scales and the 200 g weight was used to double check accuracy (99.994%). The weights were chosen so there would be one calibration point above and below the mass of the heavy holding tray, rod, and sample (approximately 135 g). Both scales operate within a range of 0 – 450 g. Calibration was originally done by the manufacturer of the electronic balance, therefore this calibration was only done to ensure accuracy.

3.1.4 Fabrication of new pellet mold and die

Two existing molds have been used to make compacted DSG pellets both with an external diameter of 30.1 mm and an overall length of approximately 50 mm. The internal diameters of the existing molds are 6.3 and 12.1 mm. The 6.3 mm mold can accommodate up to 1 g of DSG and the 12.1 mm mold can accommodate up to 3.5 g. The cylindrical dies used to compress the DSG samples inside the molds had a diameter of 6.15 and 11.90 mm respectively. Because of the relatively large difference between internal mold diameter and die diameter compressing with higher pressures sometimes resulted in some DSG being squeezed up through the inside of the mold and getting stuck to the die. This would result in mass loss, as well as increased friction between the die and mold which could have also led to the improper force being applied to the sample.

The new fabricated mold can be seen in Fig 3.5. It is made of steel with an external and internal diameter of 30.1 and 12.1 mm respectively. The overall length of the new mold is 80 mm which allows for up to 4.2 g of DSG to be compacted at once. The top of the mold is flanged in order to allow for easier insertion of the sample as well as the cylindrical die. The new

cylindrical die that was fabricated has a diameter of 12.05 mm and a length of 84.8 mm. With the new die only having a 0.05 mm smaller diameter than the mold there was no DSG sample that came up between the die and the mold during compression at 60.3 MPa.

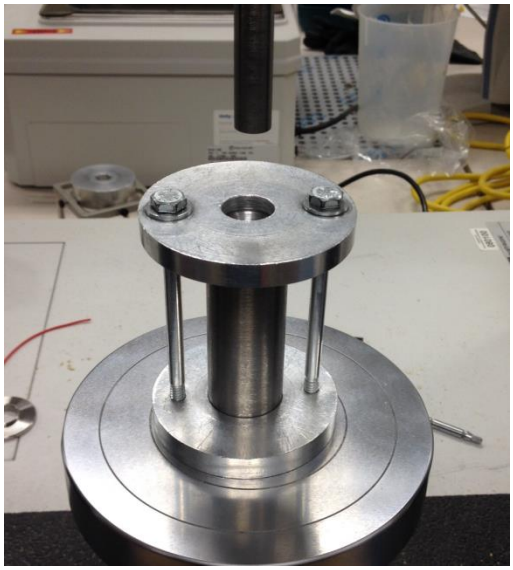

Figure 3.5. Newly fabricated cylindrical die and mold

3.2 Initial condensation experiments with wood pellets and Teflon

To determine the effect of temperature and SS velocity on the initial condensation period associated with SS drying two inert materials were chosen, poplar wood dowels and Teflon. Poplar wood was chosen because of its low thermal conductivity and low initial moisture content which would create a relatively long condensation period when drying in SS, especially at low temperatures. Teflon was also chosen for its low thermal conductivity in addition to its ability to not absorb any moisture (in the form of condensation), which would make any mass changes recorded directly related to the amount of moisture present on the sample.

For the Teflon sample, a sphere with a mass of 150 g and diameter of 50 mm was subjected to SS drying at 120 °C and 1.0 m/s for 150 s. The mass of the thin steel rod was approximately 32 g. Mass changes were recorded and can be seen in Fig. 3.6. The initial drop in mass for the first 10 s was due to the increased pressure inside the SS drying chamber causing an increase in the lifting force acting on the Teflon sphere. Furthermore, it was observed that condensation was dripping off the sphere when it was removed from the drying chamber. Therefore, the mass changes did not accurately reflect the initial condensation period for the Teflon sample.

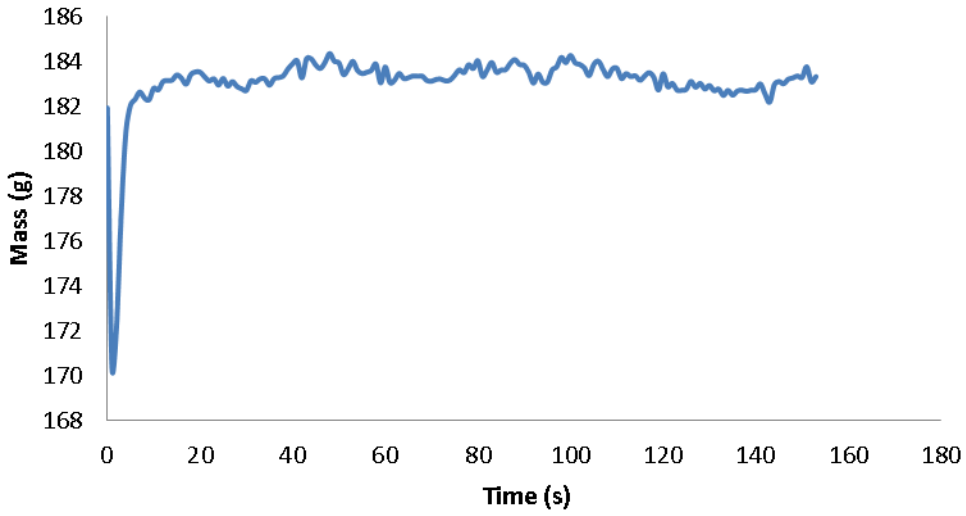

Figure 3.6. Raw data obtained from initial condensation experiment with Teflon sphere processed in SS at 120 °C and 1.0 m/s

For the wood pellet samples, a holding hanger was fabricated out of copper wire as can be seen in Fig. 3.7. There was no need for a mesh bottom because the wood pellets would not disintegrate as compared to DSG. Copper was chosen for its high thermal conductivity which

would make the initial condensation period on the holding hanger alone very short. The copper holding hanger was attached to the thin steel rod inside the drying chamber as mentioned in section 3.1.3.

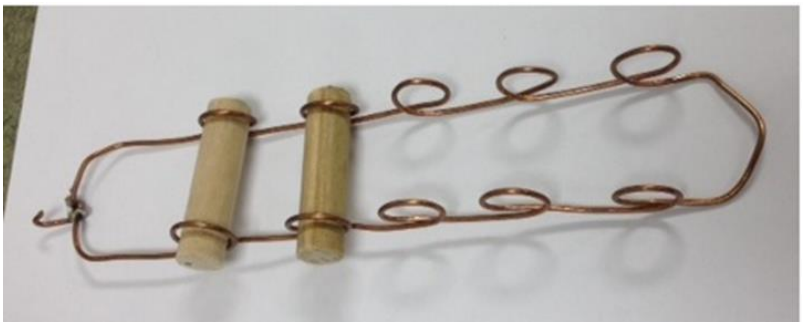

Figure 3.7. Holding hanger fabricated for poplar wood dowels

A poplar wooden dowel with a diameter of 12.7 mm was cut into pieces that were approximately 50 mm long. The two ends of the dowel were cut off and discarded since they had been painted by the manufacturer for identification purposes. The initial moisture content of the poplar wood was determined to be 6.6 ± 0.2% wb by the air-oven drying method at 103 °C for 24 h (ASTM D4442-07, 2007). This procedure was done in triplicate. Three samples at a time were then dried in the SS dryer at 120 °C and 1.0 m/s for 150 s. The copper holding hanger was left inside the drying chamber in between trials so that it would retain a higher temperature and be subjected to less initial condensation. This procedure was also done in triplicate.

Moisture content of the poplar wood samples after SS drying for 150 s was determined to be 8.3 ± 1.5% wb. The increase in moisture content suggests that some of the initial

condensation was being absorbed into the wood pellets and the standard deviation shows that the absorption was not very consistent.

To reduce or eliminate the absorption of moisture during condensation a new batch of wooden samples were first coated with 100% pure canola oil. The samples were submersed in the canola oil for 24 h, the excess oil was removed using a paper towel and then the samples were left to air dry for 1 h. The initial moisture content was determined to be 5.3 ± 0.4% wb using the ASTM D4442-07 (2007) standard in triplicate. The decrease in initial moisture content as compared to the uncoated samples suggests that the oil coating was working to prevent moisture from leaving the wood pellet. After drying the samples in SS at 120 °C and 1.0 m/s for 150 s the moisture content was determined to be 5.4 ± 0.6% wb. Since there was no significant change in moisture content before and after SS drying, it was assumed that the wood samples did not absorb any moisture during condensation. However, it was observed that when removing the coated wood samples from the SS dryer there was condensation present on the copper hanger which suggests that the condensation on the wood samples was dripping off the sample and not staying until the evaporation stage. Similar to the Teflon sphere, mass changes measured did not accurately reflect the initial condensation period for coated wood samples. Therefore the initial condensation period experiments were chosen to be done directly on DSG samples with generic assumptions being made as outlined in sections 3.4.2 and 3.5.

3.3 Distiller's spent grain sample preparation

3.3.1 Handling bulk distillers' spent grain

The raw material used in this study was a mixture of 90% corn and 10% wheat stillage obtained from a local distillery (Mohawk Canada Limited, a division of Husky Oil Limited, Minnedosa, MB). The raw material was kept in a freezer at -15 °C in a plastic pail sealed with a lid. Before sample preparation, the sealed plastic pail was taken out of the freezer and allowed to thaw for 2 days. The whole stillage was stirred to provide a more uniform mixture and reduce the effects of settling particles while thawing. The whole stillage was then centrifuged using a Sorvall General Purpose, RC-3 centrifuge (Thermo Scientific Co., Asheville, NC). The centrifuge operated at a relative centrifugal force of 790 × g, with four 1000 mL sample containers (filled approximately 75%) rotating at a speed of 2200 rpm for 10 min. The sample containers were then removed from the centrifuge leaving the stillage in 3 fractions as can be in seen in Fig 3.8. The thin stillage present in liquid form was poured out of the sample containers and discarded. The semi-solid solubles fraction was scooped out in thin layers using a spoon until the appearance of the material began to look like coarse grain. The solubles were placed in an airtight plastic bag and stored in the freezer at -15 °C. The remaining coarse grain fraction was also scooped out using a spoon, placed in an airtight bag and kept in the freezer at -15 °C.

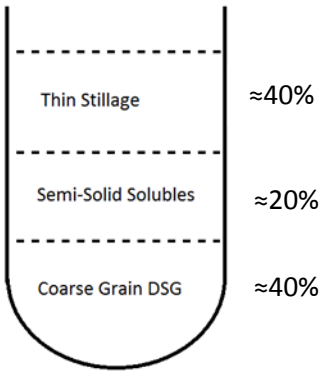

Figure 3.8. Cross section of a centrifuge sample container showing the 3 separated fractions of DSG by volume

3.3.2 Distillers' spent grain initial moisture content determination

To determine the initial moisture content of the coarse grain fraction (DSG) the airtight bag was removed from the freezer and allowed to thaw for 2 h. Moisture content was determined by the air-oven drying method according to the AACC method 44-15A (2000) by drying 2 g of wet sample at 135 °C for 2 h in a laboratory oven (Thermo Electron Corporation, Waltham, MA). This procedure was replicated 3 times. The average moisture content and standard deviation was calculated. The initial moisture content of the coarse grain fraction was 78.9 ± 0.6% wb.

3.3.3 Distillers' spent grain pellet preparation

An airtight bag of coarse grain was removed from the freezer and allowed to thaw for 2 h. Thawed sample was placed in an air-oven (Thermo Electron Corporation, Waltham, MA) at 50 °C and allowed to dry to a moisture content of approximately 30% wb. The sample was

removed from the air-oven occasionally to check the mass as well as to mix the sample. The sample was then transferred to an airtight bag. One pellet was made at a time by removing the required amount of material from the airtight bag so that when oven dried at 50 °C to a moisture content of 25% wb there would be approximately 4.2 g of sample to create a long pellet or 2.1 g of sample for a short pellet. After the sample had been dried to 25% wb it was removed from the air-oven and placed inside the cylindrical steel mold (as mentioned in section 3.1.4). If a long pellet was to be made the mold would fill completely before the entire 4.2 g of sample was used, therefore a thin steel blade was used to lightly compress the sample inside the mold until enough room had been made to accommodate the rest of the sample. The steel mold was then sandwiched in between two steel plates which were held together by two bolts. A cylindrical die with a diameter of 12.05 mm attached to a 10 kN load cell on a universal testing machine (Model 3366 Universal Testing Systems, Instron Corp., Norwood, MA) was used to make the compacted pellets by applying a load of 6820 N to the sample (equivalent to a pressure of 60.3 MPa) at a rate of 50 mm/min. After the desired load had been reached, the die was held inside the mold for 5 min in order to maintain constant pressure and prevent relaxation. After 5 min, the die was removed from the mold, the mold was removed from the steel plates and the sample was pushed out through the bottom of the mold using the cylindrical die. A vernier caliper with an accuracy of 0.01 mm was used to measure the length of the sample. An electronic balance with an accuracy of 0.001 g (Adventurer Pro AV313, Ohaus Corporation, Pine Brook, NJ) was used to measure the mass of the pellet. The difference in mass before and after pelletizing was assumed to be caused by the expulsion of water at high pressure. This assumption is supported by evidence of an oily residue left behind on the bottom

steel plate after removing the sample. In between making pellets the steel plates, inside the cylindrical mold, and cylindrical die were all wiped down with a dry paper towel. No water was used to clean the apparatus to prevent the addition of moisture in subsequent samples.

3.4 Initial condensation on the pellet surface

3.4.1 Initial condensation experiments by direct measurement

The following procedure was carried out to determine the maximum condensation, condensation time, restoration time and constant drying-rate when drying DSG pellets at 120, 150, and 180 °C with SS of velocities 1.0, 1.2, and 1.4 m/s.

Short pellets (2.1 g) were made one at a time following the procedure in section 3.3.3 and placed in separate airtight bags after recording the length with a vernier caliper and the mass with an electronic balance. After the fourth pellet had been made, all pellets were removed from the airtight bags and the length of the first pellet made was recorded again using a vernier caliper. This allowed for the maximum percentage of relaxation in the axial direction to be calculated before drying the pellets in SS. The average percentage increase in length of the first pellet made in the time it took to make the remaining three pellets was determined to be 17.7 ± 5.3%. All four short pellets were placed horizontally in the heavy holding tray described in section 3.1.3 (using 2 pins to hold each pellet in place). The pellets were then subjected to SS drying at 120, 150, or 180 °C for a total of 300 s while recording the mass of the samples and heavy holding tray. The collection of condensate procedure outlined in section 3.1.2 was conducted for each trial to determine the SS velocity. For each treatment experiments were conducted in triplicate and the average values were taken.

The raw data obtained from the data acquisition system (mass and time) was plotted. The first data point was deleted and replaced with the starting tray mass with the four short pellets. Any subsequent points that were significantly lower than the initial point were deleted due to them being affected by an increased lifting force caused by an increased chamber pressure when switching over the manual valve. On average, this resulted in the removal of the first 10 s of mass data. The lifting force was calculated by taking the average mass value of the last 70 s and subtracting it from the mass of the heavy tray and samples after drying with no SS present. The heavy tray mass was deducted and lifting force added to the raw data values to obtain the sample mass on its own. A 4^{th} power polynomial regression equation was applied and the coefficients were recorded. The mass values based on the regression equation were calculated for every time value present in the raw data and then plotted against the original regression equation to ensure accuracy. The maximum amount of condensation was calculated by taking the maximum value obtained in the regression equation and subtracting the initial sample mass. The time value associated with the maximum mass value was considered the condensation time. The time taken for the mass from the regression equation to return back to the original sample mass from the maximum condensation point was considered the restoration time. Since the samples had not been subjected to SS long enough to reach equilibrium only the mass values between 100 and 180 s of the regression equation were plotted to determine the constant drying-rate. Linear regression was applied to the cropped data and the slope of the line was recorded as the constant drying-rate in g/s. The coefficient of determination was also recorded with a minimum value of $R^2 = 0.984$ from all trials.

3.4.2 Initial condensation predictions based on measured distillers' spent grain pellet surface temperature

The T-type thermocouple used in the following experiments was calibrated by recording the temperature when the thermocouple was placed in boiling water and again when it was placed in ice water. The computer recorded values were compared to observations made using a mercury thermometer and the difference was observed to be less than 0.5 °C.

The DSG used in these experiments had a mixture of 70% coarse grain and 30% solubles. The solubles were taken out of the freezer and allowed to thaw for 2 h. The initial moisture content of the solubles fraction was determined to be 84.2 ± 0.8% wb using the AACC method 44-15A (2000) by drying 2 g of wet sample at 135 °C for 2 h in a laboratory air-oven. This procedure was conducted in triplicate. The appropriate amount of solubles was added to the coarse grain DSG fraction in order to make up 30% by mass. A single short pellet (2.1 g) was made with the mixed material using the procedure outlined in section 3.3.3. The solubles acted as a binding agent and allowed a thermocouple to be inserted into the pellet without disintegration occurring. A thin needle was inserted into one end of the pellet (in the axial direction) and was pushed through the entire length until the tip just came out of the other end. The needle was then removed and a T-type thermocouple was inserted into the hole left behind until the tip was approximately 1 mm from the outside pellet surface as can be seen in Fig. 3.9.

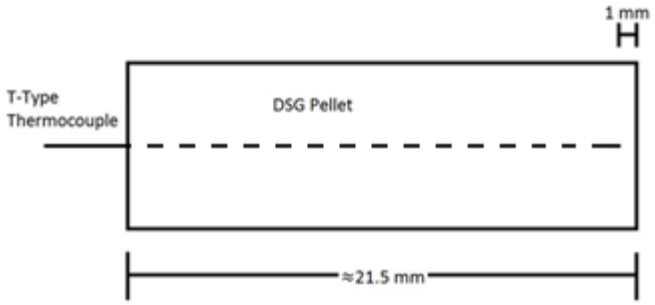

Figure 3.9. Cross section of a short DSG pellet showing the location of a thermocouple (inside pellet) for surface temperature recording

The pellet was placed horizontally inside the heavy holding tray and placed inside the SS drying chamber. A second T-type thermocouple was placed on the heavy holding tray with the tip not touching anything in order to record the SS temperature. Due to the way the computer programs are set up, the temperature recording program and the program that controls the SS system cannot be run at the same time. Therefore, while temperature recording was enabled the strip heaters surrounding the drying chamber were not operating which resulted in the chamber temperature decreasing over the entire course of drying (40 min). The temperature experiments were run at 120, 150, and 180 °C for a total of 40 min. For the initial condensation period (lasting approximately 1 – 2 min) the drop in temperature due to the strip heaters being turned off was considered negligible. The collection of condensate procedure outlined in section 3.1.2 was done for each trial to determine the SS velocity. For each temperature the target velocities were 1.0, 1.2, and 1.4 m/s. Each treatment was conducted in triplicate and the average temperature characteristic was taken. Analysis of the data obtained in order to calculate the initial condensation mass flux is outlined in section 4.1.

3.5 Temperature history experiments with added water droplet

In this experiment the goal was to determine whether a constant temperature period existed during the constant drying-rate period of SS drying of DSG with higher moisture content. A single short pellet was made using the same procedure outlined in section 3.3.3 and the same material outlined in section 3.4.2. After inserting the T-type thermocouple into the pellet a syringe was used to apply a single droplet of water onto the end of the thermocouple just inside the pellet surface. The pellet was then placed horizontally in the heavy holding tray and placed in the SS drying chamber. For these trials the pellets were only dried at 120 °C with a target SS velocity of 1.0 m/s. The collection of condensate procedure outlined in section 3.1.2 was done for each trial to determine the SS velocity. This experiment was conducted in triplicate.

3.6 Desiccator equilibrium moisture content experiments for diffusivity

Two desiccator solutions were considered to be used to keep sample parameters (moisture content and dimensions) consistent for diffusivity experiments. The first was a saturated NaCl solution with a relative humidity (RH) value of 75.5% at 20 °C and the second was a pure water solution with a RH value of 100% at 20 °C. Six long pellets were made using the procedure outlined in section 3.3.3. The mass of each pellet was recorded using an electronic balance and the dimensions were recorded using a vernier caliper. Three pellets were left in each desiccator for one week. After one week, the pellets were removed and the moisture content was determined by the AACC 44-15A (2000) air-oven drying method. The moisture content of the pellets left in the desiccator with the saturated NaCl solution was

determined to be 23.6 ± 0.3% wb. The moisture content of the pellets left in the desiccator with the pure water solution was determined to be 28.5 ± 0.8% wb. Furthermore, it was observed that the pellets kept in the desiccator with the pure water solution had visible mold on the surface which could have affected the moisture content determined.

The standard deviation calculated in the determination of the initial moisture content of the DSG fraction was 0.6% wb. Since the initial moisture content was determined to be 78.9% wb, a total of 14.93 g of wet sample would be required to have 4.2 g after drying to 25% wb. However, being one standard deviation away from the mean would result in a moisture content of 25.0 ± 2.1% wb before pelletizing. Therefore, the use of the desiccator with the saturated NaCl solution was chosen to be used for the following diffusivity and change in dimension experiments based on the lower standard deviation for moisture content.

3.7 Changes in dimensions of distillers' spent grain pellets during superheated steam drying

A set of experiments were conducted to determine the change in length and diameter of DSG pellets over the course of drying in SS. Long pellets were prepared using the procedure outlined in section 3.3.3. After pellet preparation the pellets were stored in the NaCl desiccator and left overnight. One pellet at a time was removed from the desiccator. The mass of the pellet was measured using an electronic balance, with difference in mass from the previous day being assumed to be caused by a change in moisture content. The diameter and length of the sample was also measured using a vernier caliper, and calculated as a percentage of the original pellet dimensions. Each pellet was placed horizontally in the heavy holding tray and held in place by four steel pins. The heavy holding tray was placed in the SS dryer at 120 ± 3 °C with a

steam velocity of 1.0 m/s and the sample was allowed to dry for a specific time interval (10 s, or 1, 5, 10, 20 or 60 min). The sample was then removed from the dryer and its length was recorded. The diameter was measured at 3 parallel planes (at both ends and the middle) and the average diameter was taken. The pellet was discarded after the dimensions had been recorded. The change in dimensions of the sample was calculated as a percentage of the initial dimension of the pellet after it had been in the desiccator overnight. Approximately 30 samples were initially prepared to determine the effect of SS drying on dimensional changes. Each drying time interval was conducted in triplicate and the averages were taken and plotted against time. Any pellets that experienced disintegration were not considered for dimensional change analysis. Due to the position of the steel pins for vertically oriented pellets (with respect to SS flow direction) dimensions could not be taken without removing the pellet first. Any attempt to remove vertically oriented pellets resulted in disintegration. Furthermore, the steel pins could have also restricted expansion in the axial direction. Therefore, an assumption was made that the vertically oriented pellets experienced approximately the same change in dimensions as the horizontally oriented pellets over the course of SS drying.

3.8 Diffusivity experiments

3.8.1 Diffusivity experiments with change in pellet orientation

In this set of experiments the goal was to obtain the change in mass of DSG pellets in two orientations over time as affected by SS drying at 120 °C in order to calculate effective moisture diffusivity. Long pellets were prepared using the procedure outlined in section 3.3.3. The pellets were left in the NaCl desiccator overnight. Once the drying chamber temperature

reached 120 °C the steam was diverted using a solenoid valve and two pellets with similar dimensions and moisture content were placed on the heavy holding tray connected to the electronic balance on top of the SS chamber. The pellets were kept 10 mm apart and held in position with four thin steel pins for each pellet. The steam was then diverted back to the drying chamber and a data acquisition system recorded the mass reading of the electronic balance every 3 s throughout the entire drying period. After drying in SS for 90 min, the samples were removed and placed in an air-oven at 103 °C for 24 hours to determine the final moisture content. These experiments were conducted in triplicate. Because heat and mass transfer is affected by the orientation of the sample with respect to the direction of flow of the SS drying medium, two orientations of the pellets were selected i) horizontal and ii) vertical (Fig. 3.10a, b).

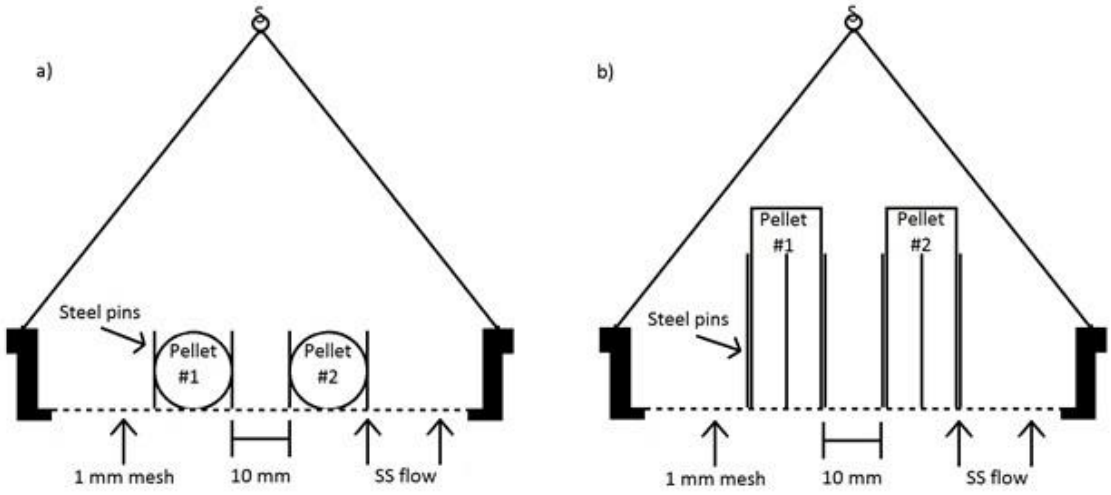

Figure 3.10. Cross section of the sample holding tray with 2 long DSG pellets oriented a) horizontally and b) vertically (Modified from Bourassa et al., 2015)

To account for the lifting force that the steam had on the holding tray and pellets, a separate set of experiments were run in triplicate for both horizontal and vertical orientation

where the steam was diverted from the drying chamber for approximately 1 min (at time intervals 2, 5, 10, 20, 30, and 40 min) and the mass of the sample was recorded. The difference in mass readings with and without the steam was considered the lifting force on the pellets and heavy holding tray. The total drying time for the lifting force experiments was 45 min. The collection of condensate procedure outlined in section 3.1.2 was done for each trial to determine the SS velocity. Analysis of the data obtained in order to calculate effective moisture diffusivity is outlined in section 4.2.

3.8.2 Diffusivity experiments with change in superheated steam temperature and velocity

In this set of experiments the goal was to obtain the change in mass of DSG pellets over time as affected by SS drying at 120, 150, and 180 °C with SS velocity of 1.0 and 1.2 m/s in order to calculate moisture diffusivity. Long pellets were prepared using the procedure outlined in section 3.3.3. The pellets were left in the NaCl desiccator overnight. Two pellets with similar dimensions and moisture contents were removed from the desiccator and placed horizontally in the heavy holding tray. The heavy holding tray was attached to the electronic balance located on top of the SS drying chamber. The samples were dried for approximately 1 h. The data acquisition system recorded the mass reading from the electronic balance every 1 s. At the end of drying, the SS was diverted and the mass of the holding tray and samples was recorded. The collection of condensate procedure outlined in section 3.1.2 was done for each trial to determine the SS velocity. After drying in SS for approximately 1 h, the samples were removed and placed in an air-oven at 103 °C for 24 h to determine the final moisture content. From the raw data collected, the average mass value from the last 70 points was calculated. The

difference in mass between the average and recorded value without SS was considered the lifting force and was added to all values. The initial mass of the holding tray was subtracted from all values. The mass corresponding to the time value of 0 s was replaced with the initial mass of both pellets combined. Any mass readings that were significantly lower than the initial mass were deleted due to the effect of an increased lifting force occurring in the first 10 s approximately. A 4^{th} power polynomial regression equation was applied and the coefficients were recorded. The dry mass of both pellets and the mass of remaining water in both pellets combined at any time Θ was calculated based on the final moisture content determined. The moisture content and MR value were back calculated for every time interval. Analysis of the data obtained in order to determine effective moisture diffusivity is outlined in section 4.2.

4 ANALYSIS

4.1 Analysis of initial condensation predictions based on measured distillers' spent grain pellet surface temperature

Eqn. 4.1 was used to predict the amount of initial condensation based on the temperature data recorded in terms of mass flux ($\dot{m}$):

$$h_f(T_{St} - T_P) = \dot{m}L \quad (4.1)$$

Where:

T_{St} is the saturation temperature of the SS under the corresponding operating pressure found from tabulated values (Khurm, 2005).

T_P is the surface temperature of the DSG pellet.

L is the latent heat of vaporization of steam at the corresponding operating pressure in J/kg found from tabulated values (Khurm, 2005).

The error associated with calculated values using Eqn. 4.1 is 0.12%.

The film condensation heat transfer coefficient (h_f) was calculated using Eqn. 4.2 (Kittiworrawatt & Devahastin, 2009):

$$h_f = 0.725\left[\frac{\rho_f(\rho_f - \rho_v)\, g\, L\, k_f^3}{d\, \mu_f\, (T_{St} - T_P)}\right]^{0.25} \quad (4.2)$$

Where:

ρ_f and ρ_v are the densities of water (condensation) and vapour, respectively.

k_f is the thermal conductivity of water found from tabulated values (Borgnakke and Sonntag, 2012).

g is the acceleration due to gravity taken as a constant 9.81 m/s^2.

d is the diameter of the pellet in m.

μ_f is the viscosity of water also taken from tabulated values (Borgnakke and Sonntag, 2012).

The above two equations were taken from a study done by Kittiworrawatt and Devahastin (2009) for low-pressure SS drying of a biomaterial. Eqn 4.2 was originally developed for film condensation but in the study by Kittiworrawatt and Devahastin (2009) the application of that equation was extended to be used during the condensation period of SS drying. Pellet surface temperature (T_P) is measured and changes during the course of the condensation period. The increase in pellet surface temperature is caused by sensible heat from the SS followed by latent heat of steam. The coefficient used in Eqn. 4.2 (0.725) was taken from Holman (2001) for a finite non-absorbing cylinder. The error associated with calculated values using Eqn. 4.2 is 0.12%.

4.2 Analysis of effective moisture diffusivity

When using SS as a drying medium it has been reported that the use of Fick's law of diffusion is appropriate to relate moisture content and drying time. Therefore, a finite cylinder model was used for effective moisture diffusivity (D_m) calculations, which has been published by Pabis et al. (1998):

$$\mathrm{MR}(\theta) = \sum_{n=1}^{\infty}\sum_{m=1}^{\infty}\beta_n\beta_m \exp[-(\mu_n^2 + \mu_m^2 K_\theta^2) Fo_{mass}] \quad (4.3)$$

The error associated with calculated values using Eqn. 4.3 is 0.19%. From Eqn. 4.3, β_n and β_m were calculated using the following equations:

$$\beta_n = \frac{4}{\mu_n^2} \quad (4.4)$$

$$\beta_m = \frac{2}{\mu_m^2} \quad (4.5)$$

$$\mu_m = (2m-1)\frac{\pi}{2} \quad (4.6)$$

$$J_0(\mu_n) = 0 \quad (4.7)$$

Where J_0 represents the Bessel function of the first kind of order zero. The value calculated for K at any time θ was found using the following equation:

$$K_\theta = \frac{R_\theta}{L_\theta} \quad (4.8)$$

Where R_θ and L_θ refer to the average radius and length of the two pellets at given time θ respectively. The error associated with calculated values using Eqn. 4.8 is 0.17%. MR(θ) is defined as the moisture ratio and is a function of time:

$$\mathrm{MR}(\theta) = \frac{M(\theta) - M_e}{M_o - M_e} \quad (4.9)$$

Where $M(\theta)$ is the average moisture content of the two pellets at given time θ after accounting for the lifting force, M_0 is the average initial moisture content of the two pellets, and M_e is the equilibrium moisture content determined experimentally. The error associated with calculated values using Eqn. 4.9 is 0.02%

Using Eqn. 4.3 with 100 terms (with both *n* and *m* ranging from 1 to 10) to calculate the Fourier number (Fo_{mass}), the effective moisture diffusivity value (D_{mass}) can be calculated:

$$D_{mass} = \frac{Fo_{mass} R_{\theta}^2}{\theta} \quad (4.10)$$

The error associated with calculated values using Eqn. 4.10 is 1.22%. Using the average MR(θ) values calculated from Eqn. 4.9, the coefficients *k* and *m* for the Page equation were found for each orientation using nonlinear regression in order to model the drying characteristic curve:

$$\mathrm{MR}(\theta) = \exp(-k\theta^m) \quad (4.11)$$

The finite cylinder model used was tested for accuracy by comparing it to an infinite cylinder model shown in Eqn. 4.12. A previously obtained set of data including MR and θ values were used, along with a pellet length of 100 m and diameter of 0.01 m. The difference between models was found to be less than 0.1%.

$$\mathrm{MR}(\theta) = \sum_{n=1}^{\infty} \frac{4}{R\,\alpha_n^2} \exp(-D_{mass}\alpha_n^2\theta) \quad (4.12)$$

The starting mass of the heavy holding tray on its own was subtracted from the mass recordings from the raw data set. The value for the lifting force was then added and a 4th power polynomial regression equation was applied. The mass values for every time value were calculated and plotted against the original regression equation to ensure accuracy. The

coefficients of the Page equation (Eqn. 4.11) were then determined using the following procedure.

The natural log of Eqn. 4.11 was taken:

$$\ln(MR) = -k\theta^m \quad (4.13)$$

If we let A = -ln(MR), Eqn. 4.13 can be rewritten as:

$$A = k\theta^m \quad (4.14)$$

Taking the natural log of both sides of Eqn. 4.14 gives:

$$\ln(A) = \ln(k) + m\ln(\theta) \quad (4.15)$$

Substituting Y_i = ln(A), X_i = ln(Θ), and b = ln(k) into Eqn. 4.15 yields:

$$Y_i = mX_i + b \quad (4.16)$$

The coefficient m can then be calculated (Lane et al.):

$$m = \frac{n\sum X_i Y_i - (\sum X_i)(\sum Y_i)}{n(\sum X_i^2) - (\sum X_i)^2} \quad (4.17)$$

The constant b can be calculated using the following equation (Lane et al.):

$$b = \bar{y} - m\bar{x} \quad (4.18)$$

Where $\bar{y}$ and $\bar{x}$ can be calculated by taking the average of all Y_i and X_i values, respectively.

After calculating b, the coefficient k can be determined:

$$k = e^{b} \tag{4.19}$$

The time values θ corresponding to a MR value of approximately 0.9, 0.8, 0.7, 0.6, 0.5, 0.4, 0.3, 0.2, 0.1, 0.05, 0.01, 0.005, and 0.001 determined from Eqn. 4.11 were recorded and used for the calculation of D_{mass} in Eqn. 4.10.

5 RESULTS AND DISCUSSION

5.1 Comparison of mass measurement before and after modifications to existing system

Before modifications were made to the existing SS system, a mass recording test was done on DSG with the original pellet mold and light holding tray. The mass of the sample used was 0.6 g with an initial moisture content of 52% wb. The results of this test can be seen in Fig. 5.1.

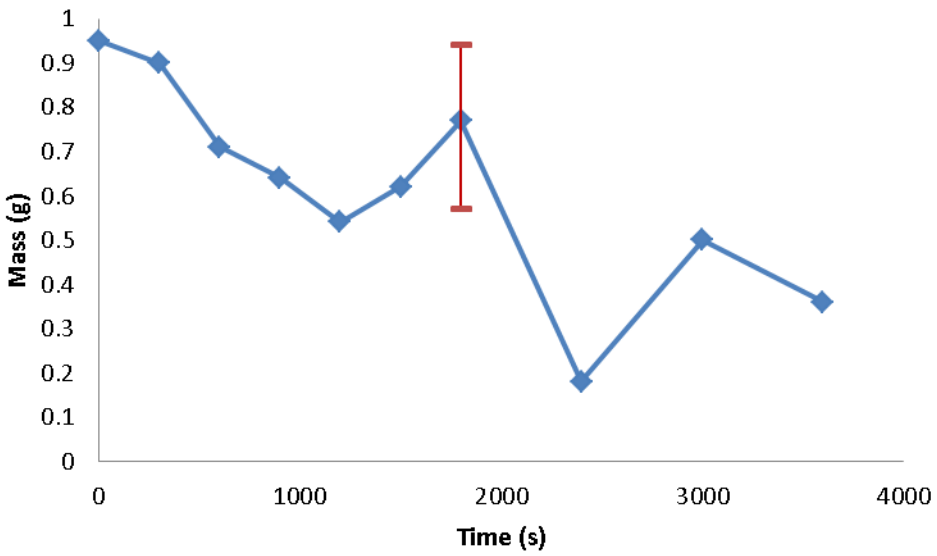

Figure 5.1. Mass changes of a DSG pellet dried in SS at 120 °C using existing mold and holding tray

Over the course of 3600 s the mass readings fluctuated significantly. The two additional data points at t = 1800 s shows the maximum and minimum values that the electronic balance was displaying. The initial mass reading is higher than the initial sample mass because the holding tray mass was not deducted and the lifting force was not accounted for at this point. The range presented by the electronic balance was equivalent to approximately 61% of the

original sample mass. Furthermore, the lowest point recorded at t = 2400 s was approximately 10% less than the dry mass of the DSG pellet. Overall, a downward trend can be observed but the level of accuracy does not allow for any type of further analysis to be done.

After making the modifications to the existing SS system, fabricating a new pellet mold and new heavy holding tray as outlined in sections 3.1.1, 3.1.3, and 3.1.4, a similar type of mass recording test was performed. The data obtained from this test (including the mass of the holding tray) can be seen in Fig. 5.2. The initial sample mass was 8.2 g.

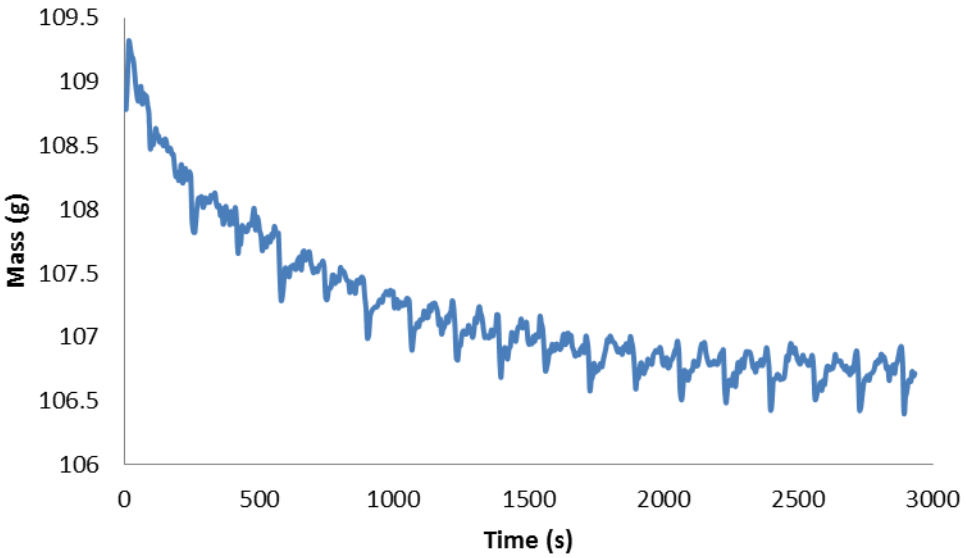

Figure 5.2. Mass changes of a DSG pellet during drying in SS at 120 °C with newly fabricated holding tray and mold

The modifications allowed for a data acquisition system to continuously record mass measurements. Fluctuations are still present in the data obtained but seem to occur in a consistent manner repeating approximately every 165 s in this case. These fluctuations could be caused by the cycle of the electric boiler supplying saturated steam to the superheater.

Therefore, a polynomial regression can be fitted in order to perform further analysis with respect to drying and diffusivity characteristics.

5.2 Initial condensation based on direct mass measurement

An example of the raw data obtained, along with the 4th power polynomial regression line applied can be seen in Fig 5.3. The initial sample mass was 8 g.

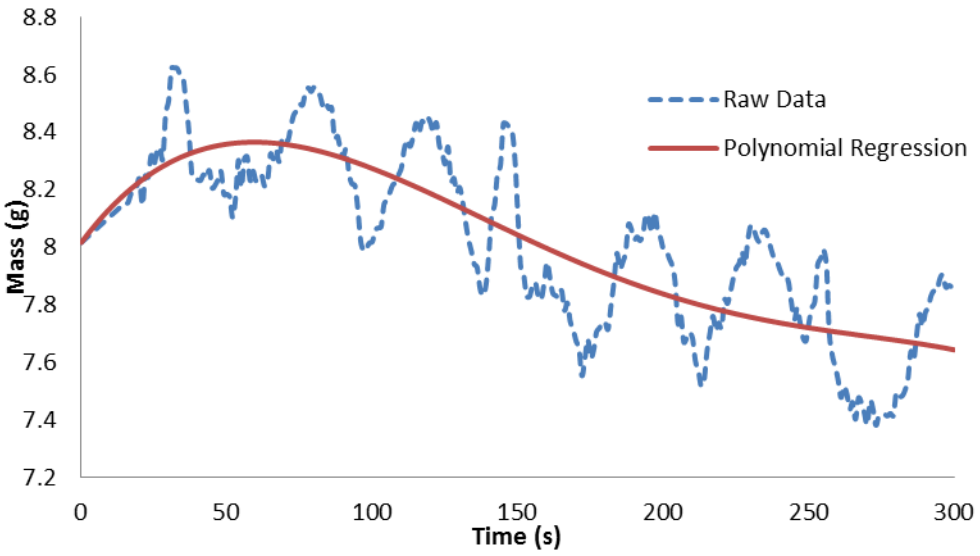

Figure 5.3. Raw data (dashed lined) with fitted 4th power polynomial regression (solid line) for DSG pellets dried in SS at 120 °C and 1.0 m/s

The average values for maximum condensation, condensation time, and restoration time for all trials are shown in Table 5.1.

Table 5.1. Average maximum condensation, condensation time, and restoration for DSG pellets dried under varying SS temperatures and velocities

SS Temperature ± 3 (°C)	SS Velocity ± 0.03 (m/s)	Maximum Condensation (g)	Condensation Time (s)	Restoration Time (s)
120	1	0.658 ± 0.034	67 ± 6	238 ± 11
	1.2	0.339 ± 0.018	55 ± 6	96 ± 8
	1.4	0.214 ± 0.015	51 ± 5	75 ± 8
150	1	0.304 ± 0.020	53 ± 6	87 ± 6
	1.2	0.134 ± 0.012	32 ± 5	39 ± 6
	1.4	0.010 ± 0.008	10 ± 4	10 ± 4
180	1	0.007 ± 0.006	7 ± 4	7 ± 4

By taking the dimensions of each pellet into account the average instantaneous mass flux for the condensation occurring on the samples surfaces can be calculated. The surface area of each pellet was calculated assuming the geometry was perfectly cylindrical and taking into account volumetric expansion. Mass flux was calculated by taking the incremental amount of condensation and dividing it by the total surface area of all four pellets. This is a useful parameter that can be used in order to compare with the predicted condensation values calculated based on measured surface temperature experiments. A comparison of calculated mass flux based on recorded mass changes with changing steam velocity at constant temperature is shown in Fig. 5.4. A comparison of calculated mass flux with changing steam temperature at constant steam velocity is shown in Fig. 5.5.

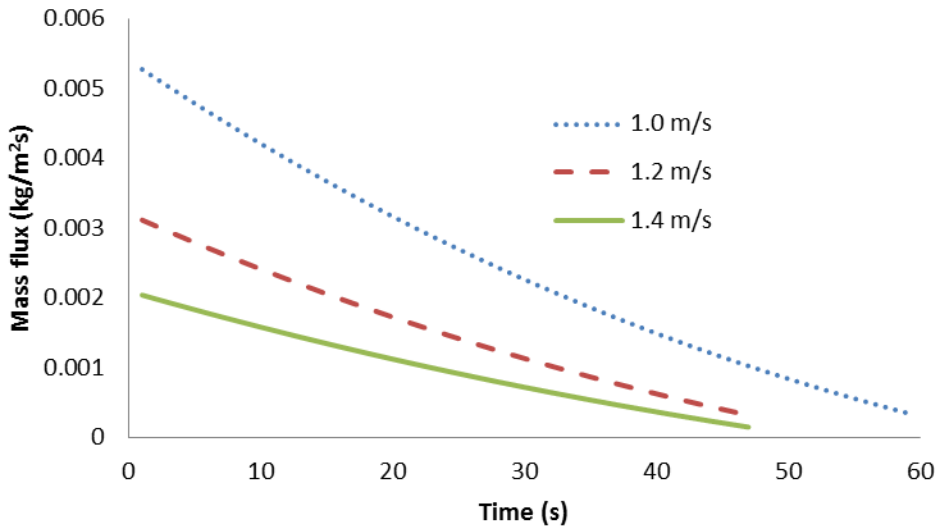

Figure 5.4. Condensation in terms of calculated mass flux based on recorded mass changes on the surface of DSG pellets dried in SS at 120 °C with three different velocities

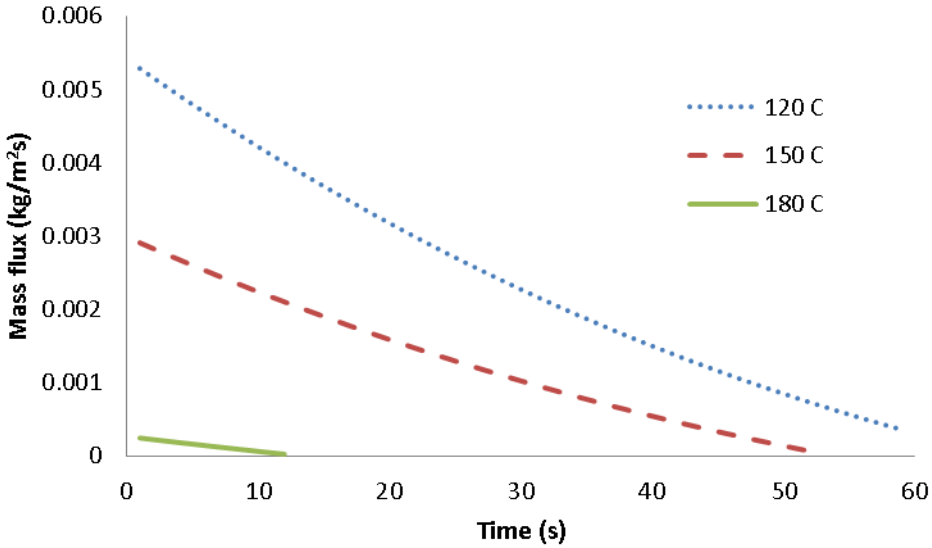

Figure 5.5. Condensation in terms of calculated mass flux based on recorded mass changes on the surface of DSG pellets dried in SS at 1.0 m/s and three different temperatures

At 180 °C there was no initial condensation calculated from one of the three trials the average was taken from, with the other two trials producing approximately 0.01 g of

condensation on a total of 4 short pellets. Therefore, the trials at higher SS velocities with a SS temperature of 180 °C were aborted, with the assumption that negligible condensation would be calculated from the data obtained. Overall, an increase in SS velocity or SS temperature resulted in a lower initial mass flux causing a decrease in initial condensation. The average condensation period for samples dried at 120 °C ranged from 67 to 51 s for SS velocities of 1.0 and 1.4 m/s, respectively. Over the same range it was calculated that there was a 67% decrease in initial condensation. For comparison, the samples dried at 150 °C experienced a 56% decrease in moisture with a SS velocity increase from 1.0 to 1.2 m/s. Furthermore, the trials performed at 120 °C and 1.2 m/s had very similar results to the trials performed at 150 °C and 1.0 m/s.

The restoration period was always calculated to be longer than the condensation period (up to 255%) except in the case of 150 °C at 1.4 m/s, and 180 °C at 1.0 m/s, where the restoration time was equal to the condensation time. Overall, the restoration time followed the same trend with an increase in SS temperature or SS velocity resulting in a decrease in restoration time.

The drying rate obtained by using the method outlined in section 3.4.1 for the constant drying-rate period for all trials are shown in Table 5.2. These values can be compared to the constant drying-rates obtained during the diffusivity experiments under similar drying conditions to ensure that the 4^{th} polynomial regression applied is representative of the correct drying characteristic. The drop in drying rate from 120 – 150 °C with an SS velocity of 1.0 m/s could have been due to one trial containing an outlier and would explain the relatively high

corresponding standard deviation. The error associated with measurement for the calculation of these values was determined to be 0.82%.

Table 5.2. Constant drying-rate (× 10^3, g/s) for varying SS temperatures and velocities

SS Chamber Temperature (°C)	SS Velocity (m/s)		
	1.0	1.2	1.4
120	4.05 ± 0.62	4.37 ± 0.45	4.39 ± 0.55
150	3.57 ± 0.93	4.63 ± 0.32	7.21 ± 0.72
180	7.73 ± 0.68	N/A	N/A

5.3 Initial condensation predicted based on measured distillers' spent grain pellet surface temperature

An example of the temperature history obtained for both the pellet surface and SS temperature can be seen in Figure 5.6. The thermocouples were positioned as outlined in section 3.4.2. The sharp increase in SS temperature at the start of the experiment is due to lag experienced by the thermocouple. Furthermore, the SS drying chamber became filled with air when the door was opened to insert the sample, and therefore at the start of the experiment the thermocouple recording the SS temperature was positioned in an air-SS mixture for a few seconds, which could have also affected the first few seconds of data.

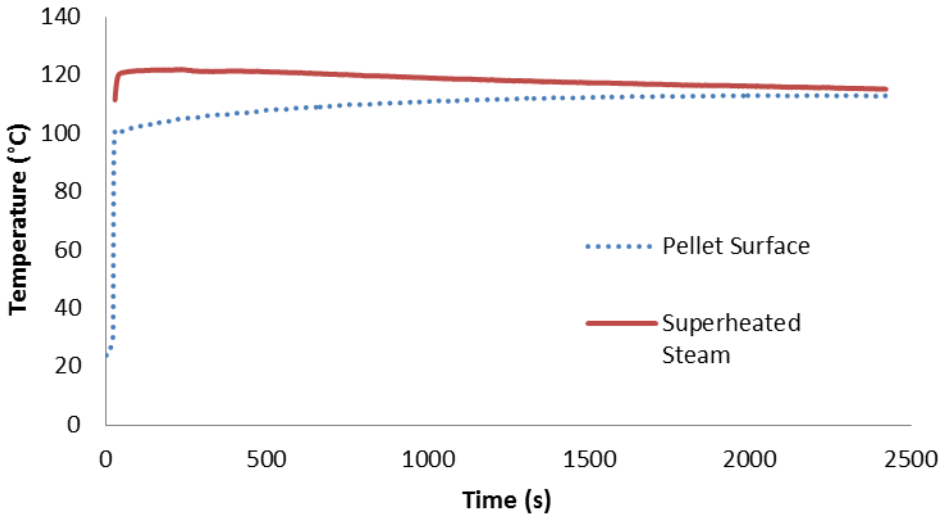

Figure 5.6. DSG pellet surface temperature during drying in SS at 120 °C and 1.0 m/s

There is a gradual increase in the surface temperature of the DSG pellet during the constant drying-rate period determined based on the drying rates calculated from the mass condensation experiments. This trend in the temperature history was also reported by Devahastin et al. (2004) for the drying of banana slices in SS and by Pronyk et al. (2010) for the SS drying of instant Asian noodles. The absence of a constant temperature period, which is normally found in hot air drying if the material is above the critical moisture point, may be caused by an exothermal process occurring during the aggregation of colloidal protein molecules during denaturation, or could also be due to the release of stored mechanical energy during pellet expansion (Fitzsimons et al. 2004; Johnson et al. 2014). The increase in temperature of the sample could also be attributed to convection taking place in the capillary pores of the DSG pellet due to a pressure gradient. A pressure gradient can be caused by the vaporization of internal water and the resistance of the DSG pellet to allow movement of that vapour (Sokolovskii, 1998).

The above hypotheses can be supported by Fig. 5.7, where a constant temperature period is observed when a water droplet has been placed on the surface of the DSG pellet prior to drying in SS. It is important to note that the SS temperature is decreasing over the course of the drying experiments due to the strip heaters being turned off in order to allow the temperature recording program on the computer to run.

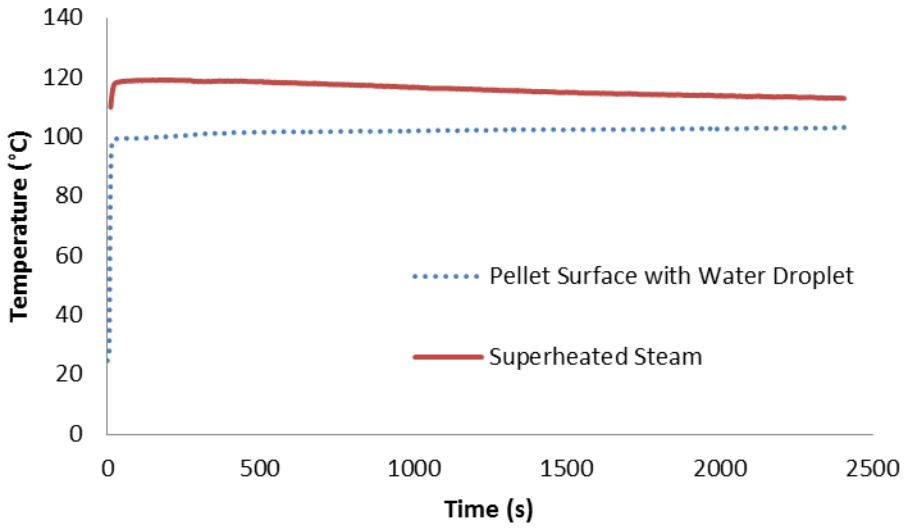

Figure 5.7. DSG pellet surface temperature with water droplet and SS profile when drying at 120 °C and 1.0 m/s

Using Eqn. 4.2, the condensation heat transfer coefficient (h_f) was calculated and is shown as a function of drying time in Figure 5.8 for constant SS temperature and varying SS velocities. The comparison of h_f at different SS temperatures with the same SS velocity can be seen in Fig. 5.9. All treatments started with an h_f value of approximately 5770 W/m^{2}K due to the DSG pellet surface temperature of all trials starting close to room temperature (22 °C). The heat transfer coefficient of the condensation increased as drying continued and reached a

maximum value at the end of the condensation period when the DSG surface temperature approached the saturation temperature of the SS.

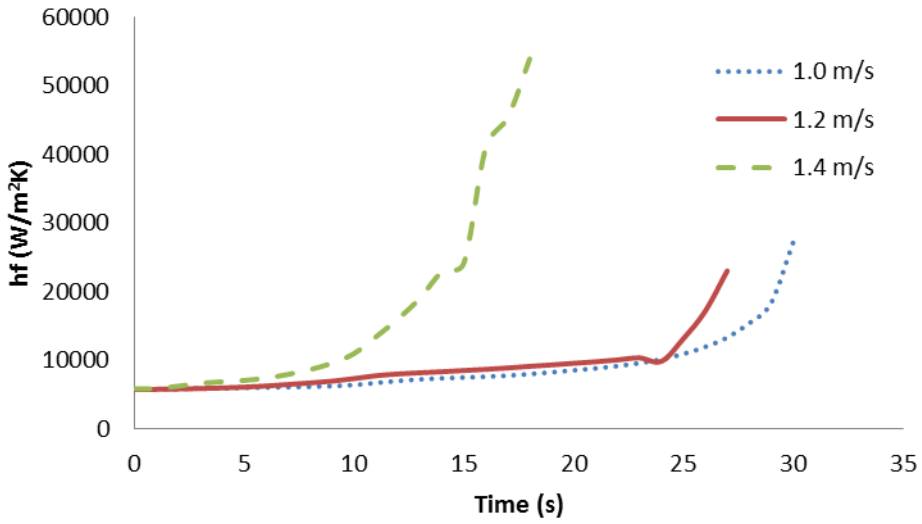

Figure 5.8. Heat transfer coefficient of condensate during the condensation period as affected by SS velocity with a temperature of 120 °C

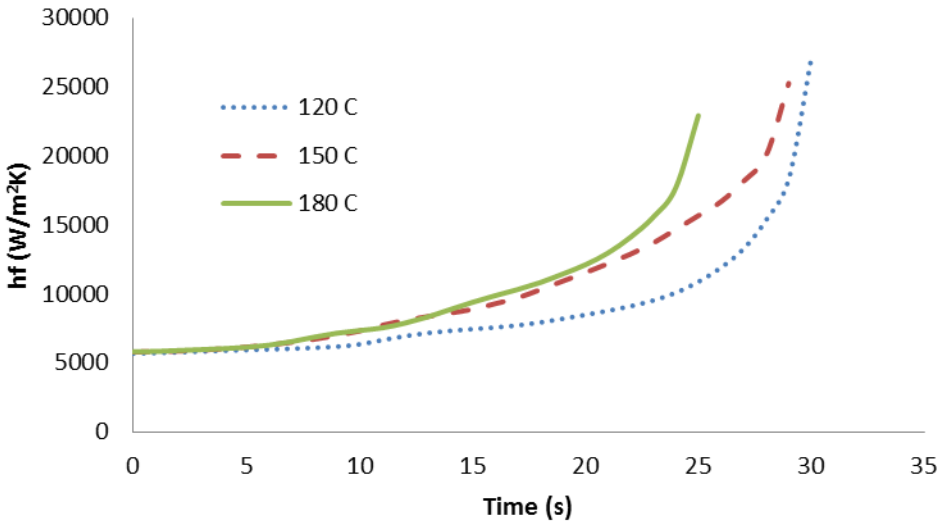

Figure 5.9. Heat transfer coefficient of condensate during the condensation period as affected by SS temperature with a velocity of 1.0 m/s

Using the values for h_f and Eqn. 4.1, the mass flux during the condensation period was calculated. Fig. 5.10 shows the comparison of mass flux with constant SS temperature and varying SS velocities. Similarly, the comparison of mass flux with varying SS temperature under constant SS velocity is shown in Fig. 5.11.

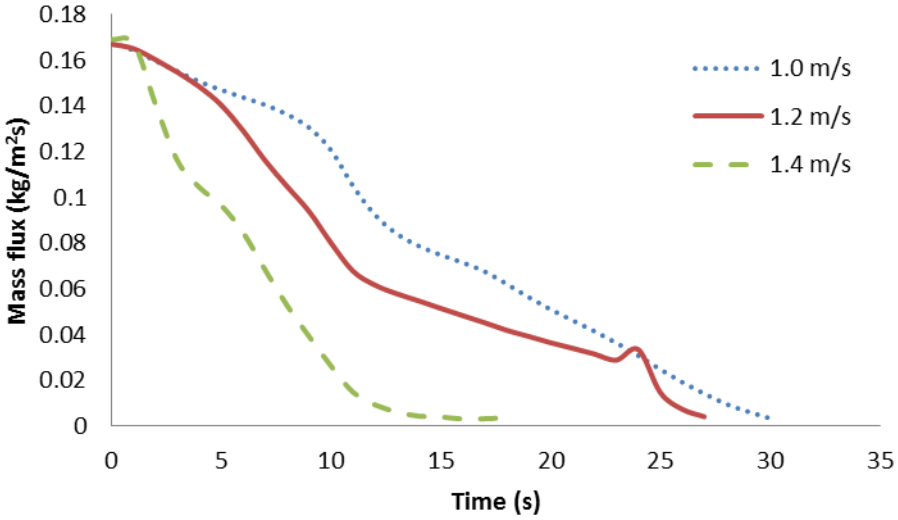

Figure 5.10. Condensation in terms of mass flux on the surface of a DSG pellet dried in SS at 120 °C with varying velocities calculated based on temperature data

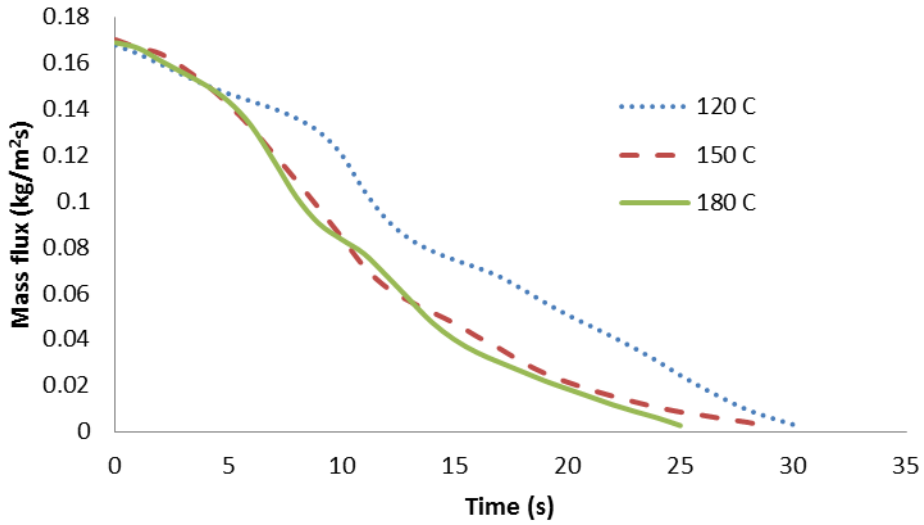

Figure 5.11. Condensation in terms of mass flux on the surface of a DSG pellet dried in SS at 1.0 m/s with varying temperatures calculated based on temperature data

Overall, the initial mass flux predicted based on measured surface temperature data was very consistent between all treatments, equal to approximately 0.17 kg/m^{2}s. The same trend was observed for condensation time as compared to the direct mass measurement experiments with an increase in SS temperature and SS velocity resulting in decreased condensation time. The increase in mass flux for the 1.2 m/s trial at approximately 25 s (in Fig. 5.10) could have been due to moisture condensing on the thermocouple inside the DSG pellet for one trial, causing the average h_f value to decrease during that period.

5.4 Comparison between direct mass measurement and predicted method based on surface temperature for determining initial condensation

In order to compare the maximum amount of condensation between direct mass measurements and predicted values based on the measured surface temperature history, linear regression was first applied to the mass flux data obtained from the experiments

measuring surface temperature (Fig. 5.10 and 5.11). The linear regression equation was then integrated over the condensation time and multiplied by the surface area of the DSG pellet. The maximum condensation values obtained from the direct mass measurements (from Table 5.1) were divided by 4 calculate the average values per single pellet in order to compare to the predicted values based on measured surface temperature history which only used a single pellet. A comparison of maximum condensation for direct mass measured values and predicted values based on surface temperature measurement is shown in Table 5.3.

Table 5.3. Comparison of maximum condensation between mass and temperature based methods per single pellet

SS Temperature ± 3 (°C)	SS Velocity ± 0.03 (m/s)	Maximum Condensation Mass Based (g)	Maximum Condensation Temperature Based (g)	Difference Between Predicted And Measured Values For Maximum Condensation (%)
120	1.0	0.165 ± 0.009	2.85 ± 0.31	1720
120	1.2	0.085 ± 0.005	2.32 ± 0.25	2730
120	1.4	0.054 ± 0.004	1.25 ± 0.14	2310
150	1.0	0.076 ± 0.005	2.15 ± 0.16	2830
150	1.2	0.034 ± 0.003	1.50 ± 0.21	4420
150	1.4	0.003 ± 0.002	0.79 ± 0.09	26200
180	1.0	0.002 ± 0.002	1.61 ± 0.16	80600

The difference calculated between the methods show that the predicted values are very different from the directly measured mass values. For the case of drying in SS at 120 °C the percentage difference between all SS velocities was relatively constant compared to the other SS temperatures. Therefore, the constant chosen for a cylindrical geometry in Eqn. 4.2 could potentially be changed in order to obtain better agreement between the directly measured values and the predicted values based on measured surface temperature. However, the very

large differences observed for the higher SS temperatures and velocities could be the result of Eqn. 4.2 not accounting for evaporation during the condensation period (Kittiworrawatt & Devahastin, 2009). Since the temperature model does not take into account evaporation during the condensation period, the condensation calculated is the sum of all moisture condensed on the DSG pellet assuming that any evaporation occurs after the maximum has been accumulated. Accounting for simultaneous evaporation and condensation during the condensation period includes modifying Eqn. 4.2 so it includes a term that is affected by the SS temperature. This should affect the h_f values calculated in section 5.3 and in turn affect the predicted mass flux with the potential to provide a better fit to the data obtained from direct mass measurements. One error that could have affected the direct mass measurement results is the amount of data used to apply the 4^{th} power polynomial regression. If a longer drying experiment were to be done the regression would be influenced by the later data points that may not have been present in this study. The result would be a decrease in maximum initial condensation, condensation time, and constant drying-rate. Furthermore, any condensation that dripped off of the sample or holding tray would have resulted in an observed mass loss which would have also affected the regression applied.

5.5 Change in dimensions of a distillers' spent grain pellet over the course of drying in superheated steam

The average percentage change in length of a DSG pellet as a function of moisture content is shown in Fig. 5.12.

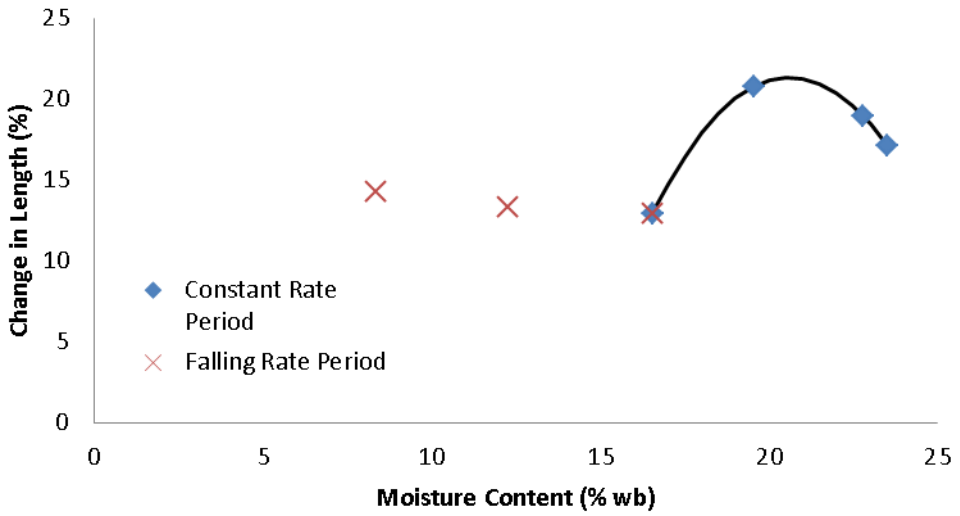

Figure 5.12. Average percentage change in length of horizontally oriented DSG pellets dried in SS at 120 °C

The increase in length of the compacted DSG pellets when subjected to SS drying can be attributed to the relaxation of stress stored during pelletizing. The compacted pellets immediately began to expand when they came in contact with SS. During the condensation period a slight rise in temperature (as seen in Fig. 5.6) was observed followed by a more rapid increase in temperature during the restoration and constant drying-rate period. The increasing temperature can affect the stress relaxation caused by the elastic extension of the polymer matrix as reported by Johnson et al. (2014). Later in the constant drying-rate period and into the falling drying-rate period a decrease in moisture content of the DSG pellet causes a relative decrease in the length of the pellet. This trend is in agreement with Simal et al. (1998) who reported that the shrinkage of their samples during drying was proportional to its moisture content. Average percentage change in length of a DSG pellet with respect to decreasing moisture content during the condensation and constant drying-rate periods was accurately represented with a 2^{nd} order polynomial regression equation (R^2 = 0.997). During the falling

drying-rate period, the percentage increase in length was calculated to be 13.5 ± 0.7% with respect to the average initial length of the pellets after removing it from the desiccator containing the saturated NaCl solution.

The average percentage change in diameter of a DSG pellet as a function of moisture content is shown in Figure 5.13. The results of statistical analysis showed that the lateral strain is insignificant with respect to moisture content ($P \leq 0.22$). Therefore, the average percentage change in diameter of compacted pellets during the entire course of SS drying was calculated to be an increase of 3.9 ± 0.5%. The average initial diameter of the pellets after being in the desiccator was 13.18 ± 0.22 mm.

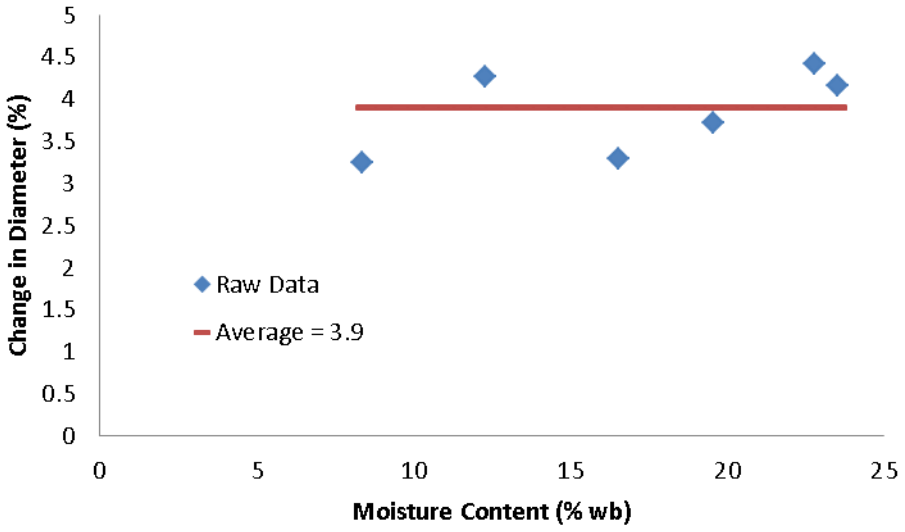

Figure 5.13. Average percentage change in diameter of horizontally oriented DSG pellets dried in SS at 120 °C

5.6 Effective moisture diffusivity and drying characteristics based on orientation

The drying characteristics developed based on the Page equation (Eqn. 4.11) of the DSG pellets both in horizontal and vertical orientations are shown in Fig. 5.14. The constant drying-rate period lasted for approximately 50 s for the vertical orientation as compared to the horizontal orientation which lasted closer to 525 s. A linear regression trend line was chosen for the drying curves with a coefficient of determination value of at least 0.999 to represent the constant drying-rate period.

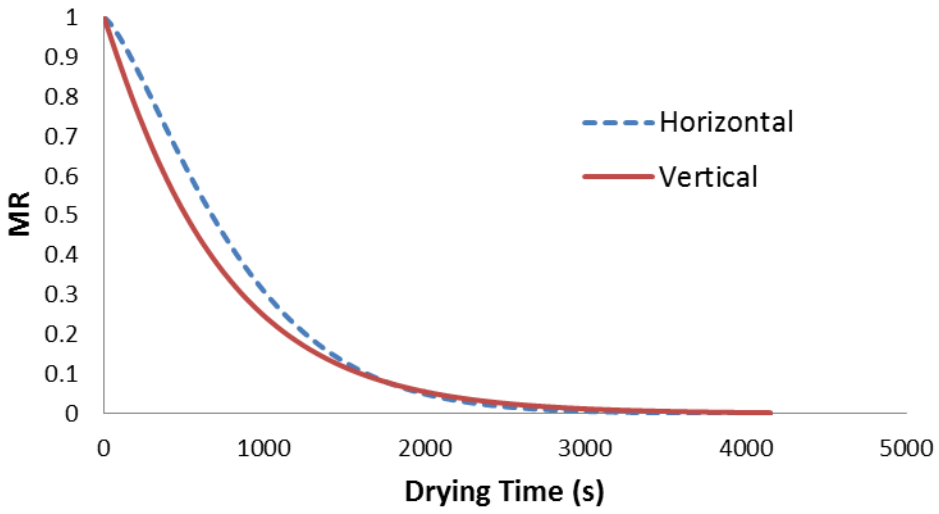

Figure 5.14. Drying characteristics based on Page equation for DSG pellets dried in SS at 120 °C with differing orientation

The initial accelerated drying of the DSG pellets in the vertical orientation could have been caused by the larger surface area that came in direct contact with the SS in comparison to the DSG pellets dried in the horizontal orientation. The difference in the blockage ratio (the ratio of frontal surface area of the DSG pellet to the cross sectional area of SS flow in the drying chamber) in each orientation would cause a change in the Nusselt number (Lavasani &

Maarefdoost, 2014). Therefore, for the same SS velocity with a Reynolds number that is approximately constant, the blockage ratio of DSG pellets oriented vertically will be lower than that of the horizontally oriented pellets. The result is a higher heat transfer rate in the condensation and constant drying-rate period for vertically oriented pellets as compared to horizontal pellets. Both orientations reached the same moisture content value at approximately 1700 s and followed the same characteristic for the remainder of the falling drying-rate period. Equilibrium moisture content was calculated to be 3.8% wb and was attained after approximately 2500 s. The coefficients for the Page equation (Eqn. 4.11) for the horizontal drying experiments were calculated to be $k = 1.05 \times 10^{-4}$ and $m = 1.35$ and for the vertical drying experiments were calculated to be $k = 1.01 \times 10^{-3}$ and $m = 1.05$ when θ is in s.

The effective moisture diffusivity of the DSG pellets calculated based on Eqn. 4.10 for both horizontal and vertical orientations is shown in Fig. 5.15. The effective moisture diffusivity values for horizontally oriented pellets ranged from 4.08×10^{-10} to 1.07×10^{-8} m^2/s. The effective moisture diffusivity values for vertically oriented pellets ranged from 6.53×10^{-10} to 1.14×10^{-8} m^2/s. The diffusivity values for both orientations were within the general range for food materials (Rafiee et al., 2010). Effective moisture diffusivity began to decrease once the moisture content went below approximately 3.9% wb. Statistical analysis showed that there was no significant effect ($P \leq 0.84$) of orientation on the overall effective diffusivity characteristics. Furthermore, the maximum values of effective diffusivity that occur at approximately 3.9% wb are not significantly different due to the standard error being 4.93×10^{-9} m^2/s. Therefore, it can be concluded that the diffusivity coefficient of DSG pellets dried in SS is independent of pellet orientation. However, when only the constant drying-rate period is

considered, the effective moisture diffusivity profile was found to be significantly different ($P<0.0015$) with respect to change in orientation of the DSG pellets. At the start of the constant drying-rate period the transfer of energy is primarily in the form of convective heat transfer, which is higher for vertically oriented pellets due to the lower blockage ratio. As the drying process reaches the later phase of the falling drying-rate period, the point when the moisture content of the DSG pellets approach equilibrium, the heat from the SS transfers through the surface towards the core of the pellet. At this stage, the blockage ratio does not have an effect and effective diffusivity is independent of orientation at this stage. The drop in effective moisture diffusivity at lower moisture contents is in agreement with a study done by Aguerre & Suarez (2004) on corn, manioc, and potatoes where a decrease in D_{mass} occurred below a moisture content of 0.1 db (dry basis).

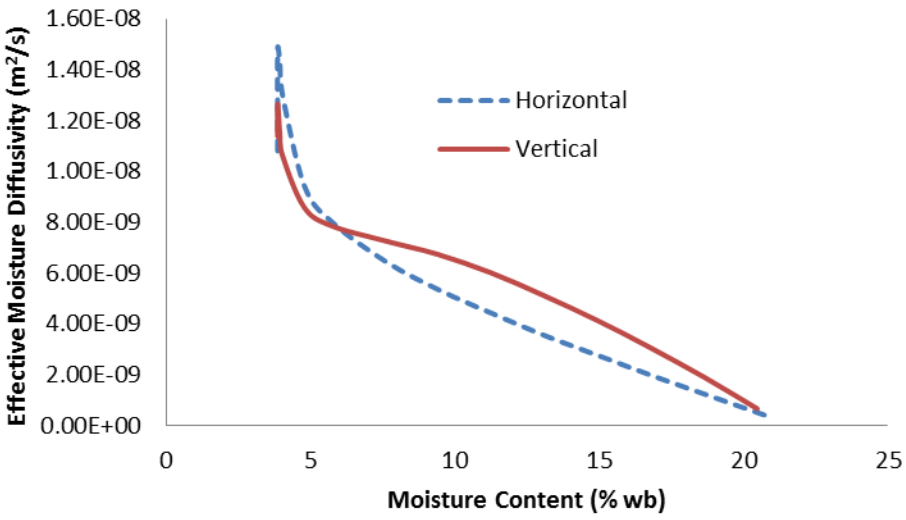

Figure 5.15. Effective moisture diffusivity for DSG pellets dried in SS at 120 °C with differing orientation

The diffusivity coefficient was calculated as the average of the effective diffusivity values obtained and determined to be 6.96×10^{-9} m^2/s for vertically oriented DSG pellets, and 6.86×10^{-9} m^2/s for horizontally oriented pellets. These values are in close agreement with a difference of only 1.4 %, however they should be used with caution since a larger number of effective moisture diffusivity values were calculated for MR values less than 0.1. Another method to determine the diffusivity coefficient would be to take the geometric mean of the data which indicates central tendency. Using this method the diffusivity coefficients were calculated to be 5.57×10^{-9} m^2/s for vertically oriented DSG pellets, and 4.73×10^{-9} m^2/s for horizontally oriented pellets.

5.7 Effective moisture diffusivity and drying rates based on changes in superheated steam temperature and velocity

For this set of experiments, the SS velocity factor of 1.4 m/s was excluded for SS temperatures of 120 and 150 °C. In order to achieve a SS velocity as high as 1.4 m/s the pressure in the pipe transferring the SS to the drying chamber needed to be maintained at approximately 3.0 psi (20.7 kPa). Once this pressure had been reached, diverting the manual valve from the water reservoir back to the drying chamber caused a significant increase in chamber pressure (upwards of approximately 2.5 psi, or 17.2 kPa) which resulted in the rubber seal on the chamber door to eventually fail. Therefore, it was determined that running drying experiments at 1.4 m/s posed a safety concern, was very hard on the SS system, and could potentially disintegrate the DSG pellets. Again, only the 1.0 m/s SS velocity was chosen for a SS temperature of 180°C.

An example of the raw data obtained along the 4th power polynomial regression and regression values calculated with 4 significant digits is shown in Fig. 5.16.

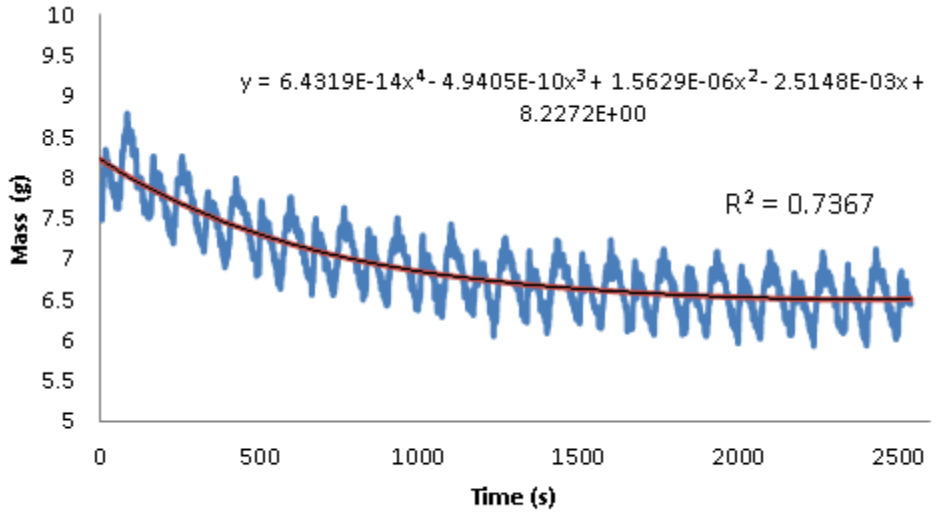

Figure 5.16. Example of raw data (zigzag line) obtained and 4th power polynomial regression applied when drying DSG pellets in SS at 120 °C and 1.0 m/s

The average effective moisture diffusivity values for DSG pellets dried at 120, 150, and 180°C with a SS velocity of 1.0 m/s is shown in Fig. 5.17.

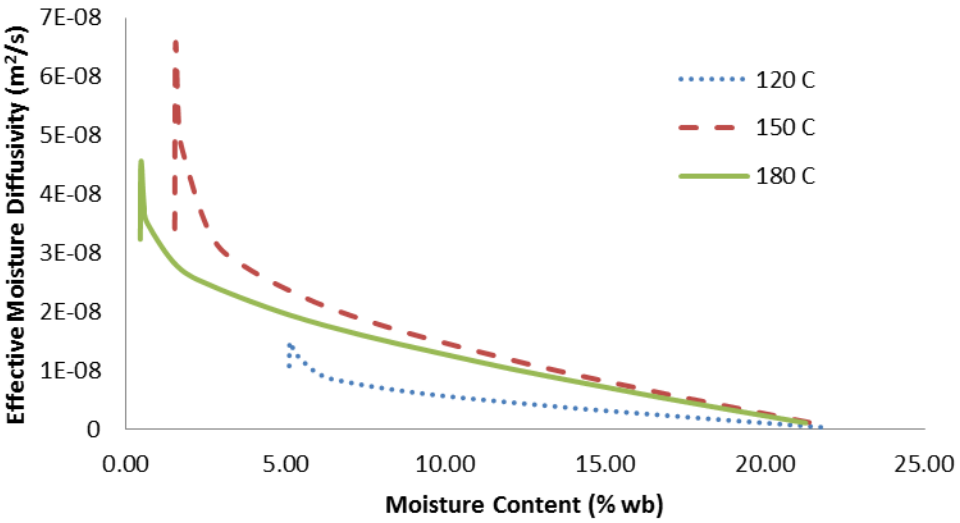

Figure 5.17. Effective moisture diffusivity characteristics of DSG pellets dried in SS at 1.0 m/s and varying temperatures

All trials experienced a decrease in effective moisture diffusivity as the samples approached their respective EMC. For samples dried at 120 °C, the EMC was determined to be 5.1 ± 0.4% wb as compared to 0.5 ± 0.1% wb for samples dried with an SS temperature of 180 °C. Overall, there was no observable effect of SS temperature on effective moisture diffusivity.

Fig. 5.18 shows the average effective diffusivity for DSG pellets dried at 120 °C with a SS velocity of 1.0 and 1.2 m/s. Similarly Fig. 5.19 shows the average effective diffusivity for trials performed at 150 °C with SS velocities of 1.0 and 1.2 m/s.

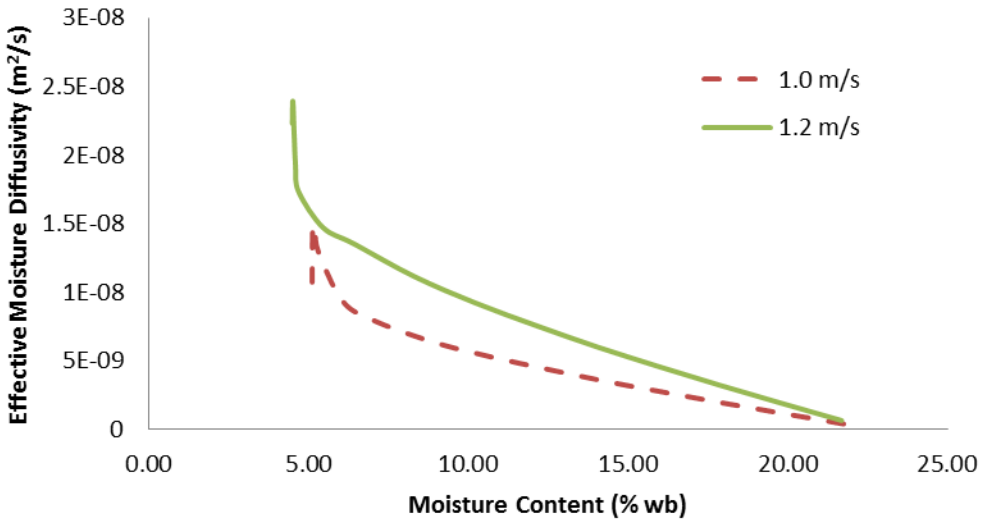

Figure 5.18. Effective moisture diffusivity characteristics of DSG pellets dried in SS at 120 °C with varying velocities

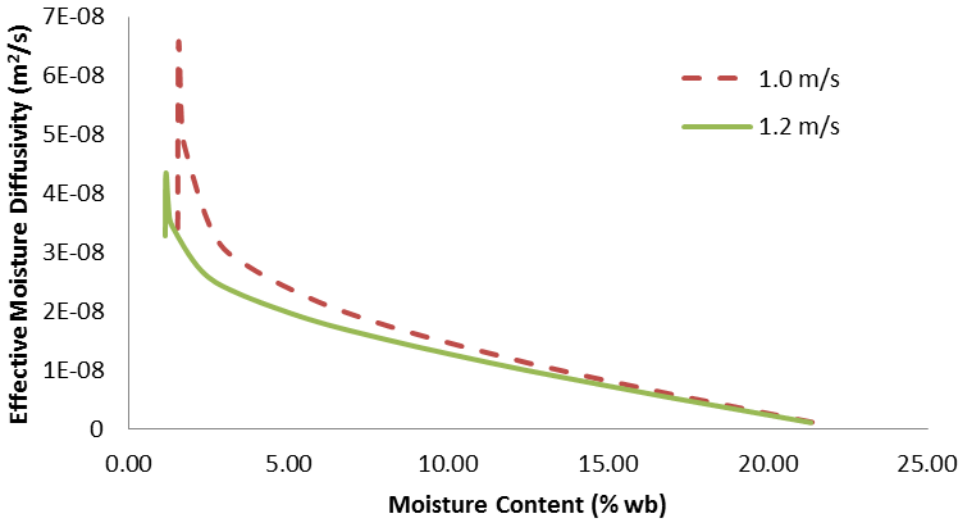

Figure 5.19. Effective moisture diffusivity characteristics of DSG pellets dried in SS at 150 °C with varying velocities

Similarly, there was no observable effect of SS velocity on effective moisture diffusivity as the average values were higher at 1.0 m/s than 1.2 m/s with an SS temperature of 150 °C but the opposite trend was observed for 120 °C. Increasing the SS velocity should increase the drying rates observed during the constant drying-rate period. Therefore, the effective moisture diffusivity should be increased during the constant drying-rate period due to the lower time value for corresponding MR values. In this case the constant drying-rate periods were determined to be relatively short in which case the effective moisture diffusivity characteristics were calculated primarily in the falling drying-rate period and are expected to be consistent with a change in SS velocity. Furthermore, the two velocities chosen for analysis were relatively close and the equipment used to record the data required for diffusivity analysis may not have been accurate enough to determine such a difference. Since there was no observable effect of SS temperature or velocity on effective moisture diffusivity, the diffusivity coefficient was calculated to be 1.56×10^{-8} m^2/s by taking the average values from all treatments. Again this value should be used with caution since a large number of effective diffusivity values were calculated with a corresponding MR value less than 0.1. Using the geometric mean, the diffusivity coefficient was calculated to be 1.05×10^{-8} m^2/s.

The constant drying-rate period for each trial was determined based on applying a linear trend line that had a coefficient of determination value of at least 0.999. The average of these values were taken for each treatment and are shown alongside the constant drying-rates obtained from the initial condensation experiments based on mass recording in Table 5.4.

Table 5.4. Constant drying-rates and comparison to rates obtained from initial condensation experiments

SS Temperature ±3 (°C)	SS Velocity ±0.03 (m/s)	Constant Drying-Rate ($\times 10^3$, g/s)	Difference In Rates Obtained In Section 3.2 (%)
120	1.0	1.98 ± 0.28	51.1
120	1.2	2.43 ± 0.14	44.3
150	1.0	3.62 ± 0.27	1.6
150	1.2	3.80 ± 0.23	17.9
180	1.0	4.26 ± 0.12	44.9

The inconsistent difference in drying rates obtained between mass based initial condensation experiments and effective diffusivity experiments could have been caused by a difference in total drying time. Extending the drying time for the initial condensation experiments would have caused the 4^{th} power polynomial regression to be flattened, resulting in a lower maximum condensation and lower constant drying-rate which would reduce the difference in rates observed in Table 5.4.

6 CONCLUSIONS

Parameters associated with the condensation period, such as the maximum condensation, condensation time, and restoration time were determined from direct mass measurements of DSG pellets dried under different SS temperatures (120, 150, and 180 °C) and velocities (1.0, 1.2, and 1.4 m/s). An increase in SS temperature from 120 to 180 °C resulted in a decrease of 97% in maximum condensation and an 84% decrease in condensation time when the SS velocity was 1.0 m/s. An increase in SS velocity from 1.0 to 1.4 m/s when the SS temperature was 120 °C resulted in a decrease of 67% in maximum condensation and a 24% decrease in condensation time. The condensation period was also modeled based on measured DSG pellet surface temperature data and compared to the direct mass measurement values. In general the two methods showed very different results with respect to the maximum condensation calculated. However, the predicted model based on measured DSG surface temperature did not account for simultaneous evaporation and condensation which could have led to an overestimation of moisture condensation present on the surface of the DSG pellet.

The effective moisture diffusivity of a DSG pellet was determined using a finite cylinder model and accounting for volumetric shrinkage. For DSG pellets dried in SS at 120 °C, it was determined that the orientation of the pellet (horizontal or vertical) did not have a significant effect on the overall effective moisture diffusivity. However when the effective moisture diffusivity profile was broken down into the constant drying-rate and falling drying-rate periods it was determined that there was a significant effect of orientation ($P<0.0015$) during the constant drying-rate period.

For DSG pellets dried horizontally, the effective moisture diffusivities were calculated for differing SS temperatures (120, 150, and 180 °C) and velocities (1.0 and 1.2 m/s). There was no significant effect of either SS temperature or velocity on the effective moisture diffusivities determined. All treatments showed a decrease in effective moisture diffusivity as the DSG pellets approached their respective EMC values based on the operating SS temperature. The diffusivity coefficient, taken as the average of all effective moisture diffusivity values, was determined to be 1.56×10^{-8} m^2/s. Using the geometric average, the diffusivity coefficient was determined to be 1.05×10^{-8} m^2/s.

7 RECOMMENDATIONS FOR FUTURE RESEARCH

In general, overall improvements to the existing SS system can be continued to be made. The source for the consistent fluctuations observed in the raw mass recordings could be investigated. If the mass fluctuations cannot be avoided, experiments could be run to determine a regression model to account for changes in lifting force during mass recording. A second larger chamber could be installed before the drying chamber which could potentially reduce the pressure fluctuations observed inside the chamber, especially at the start of experiments.

For experiments looking into the initial condensation period it would be beneficial to determine a standard method for applying regression to the raw data obtained. If the experiments were to be run for a longer period of time any regression applied would reduce the maximum condensation and condensation time. Therefore, analysis of the condensation period would seem to be a function of the SS drying time instead of the SS temperature and velocity. Furthermore, incorporating some type of video recording device might help to observe the initial condensation period in order to look for condensation occurring on the holding tray, as well as any condensation that may be dripping off the samples which would otherwise be recorded as mass loss. For analysis based on temperature profiles, accounting for evaporation during the condensation period could result in a better match with the mass based model.

For experiments that look into the effective moisture diffusivity of samples dried in SS some analysis could be done in order to determine how many terms should be used for finite geometry equations in order to reduce the amount of work going into data analysis while at the

same time not affecting accuracy of the results. For the finite cylinder model 100 terms were used for simplicity; however because of the double summation in Eqn. 4.3 the coefficients for the later terms (when *n* and *m* are both large) became negligible. When either *n* or *m* was large and the opposite term was small the coefficient was large enough that is should still be accounted for. Therefore, a model where *n* = 1 and *m* ranges from 1 to 10, *n* = 2 and *m* ranges from 1 to 9, etc., could reduce the amount of terms by 50% while possibly not affecting the accuracy of the calculated effective moisture diffusivity. Another improvement would be to develop a computer program that could take inputs such as drying time, MR, initial length, initial diameter, volumetric shrinkage coefficients, and final moisture content and automatically determine the effective moisture diffusivity vs. moisture content profile. This would save time when analyzing data since the method used in this study required the pellet length and diameter to be determined at each time interval and then plugged into the finite cylinder model to calculate the effective moisture diffusivity for one specific MR value and then repeat all steps to calculate the next value for effective moisture diffusivity.

Aside from experimental set-up and analysis future research could include developing a computer simulation of the entire drying process. The results obtained in this study could help towards validating simulations that could be run on such a computer program. If DSG were to be modelled specifically, other properties such as thermal conductivity and specific heat would probably have to be obtained in order to accurately develop such a simulation. Since the pellets in this study were all made using the same pressure, an effect of density on thermal conductivity would have to first be investigated if other pressures were to be used.

REFERENCES

AACC Method 44-15A. 2000. Moisture-air-oven methods. In: *Approved Methods of the American Association of Cereal Chemists.* St. Paul, MN.

ASTM D4442-07. 2007. Standard test methods for direct moisture content measurement of wood and wood-based materials. In: *ASTM International.*

Aguerre, R.S., and C. Suarez. 2004. Diffusion of bound water in starchy materials: application to drying. *Journal of Food Engineering* 64(1): 389 – 395.

Ayoade, D.J., E. Kiarie, B.A. Slominski, and C.M. Nyachoti. 2014. Growth and physiological responses of growing pigs to wheat-corn distillers dried grains with solubles. *Journal of Animal Physiology and Animal Nutrition* 98(3): 569 – 577.

Barchyn, D. 2015. Integration of solar energy into a superheated steam process stream for the pre-treatment of lignocellulosic biomass. Unpublished master's thesis, University of Manitoba, Department of Biosystems Engineering, Winnipeg, Canada.

Bonnardeaux, J. 2007. Potential uses for distillers grain. In Compilation by the Department of Agriculture and Food. Western Australia.

Borgnakke, C., and R.E. Sonntag. 2012. Fundamentals of Thermodynamics. Wiley (8^{th} ed.). Print.

Bourassa, J., R.P. Ramachandran, J. Paliwal, and S. Cenkowski. 2015. Drying characteristics and moisture diffusivity of distillers' spent grains dried in superheated steam. *Drying Technology.* In Press.

Cenkowski, S., M.E. Sosa-Morales, and M.C. Flores-Alvarez. 2012. Protein content and antioxidant activity of distillers' spent grain dried at 150°C with superheated steam and hot air. *Drying Technology: An International Journal* 30(11): 1292 – 1296.

Cenkowski, S., C. Pronyk, D. Zmidzinska, and W.E. Muir. 2007. Decontamination of food products with superheated steam. *Journal of Food Engineering* 83(1): 68 – 75.

Cromwell, G.L., K.L. Herkelman, and T.S. Stahly. 1993. Physical, chemical, and nutritional characteristics of distillers dried grains with solubles for chicks and pigs. *Journal of Animal Science* 71(3): 679 – 686.

Da Silva, W.P., C. Silva, and J.P. Gomes. 2013. Drying description of cylindrical pieces of banana in different temperatures using diffusion models. *Journal of Food Engineering* 117(1): 417 – 424.

Da Silva, W.P., C.M. Silva, D.D. Silva, and C.D. Silva. 2008. Numerical simulation of the water diffusion in cylindrical solids. *International Journal of Food Engineering* 4(2): 1 – 16.

Devahastin, S., P. Suvarnakuta, S. Soponronnarit, and A.S. Mujumdar. 2004. A comparative study of low-pressure superheated steam and vacuum drying of a heat-sensitive material. *Drying Technology: An International Journal* 22(8): 1845 – 1867.

Efremov, G., M. Markowski, I. Bialobrzewski, and M. Zielinska. 2008. Approach to calculation time-dependent moisture diffusivity for thin layered biological materials. *International Communications in Heat and Mass Transfer* 35(1): 1069 – 1072.

Elustondo, D.M., A.S. Mujumdar, and M.J. Urbicain. 2002. Optimum operating conditions in drying foodstuffs with superheated steam. *Drying Technology: An International Journal* 20(2): 381 – 402.

Erdogdu, F., and M. Turhan. 2006. Analysis of dimensional ratios of regular geometries for infinite geometry assumptions in conduction heat transfer problems. *Journal of Food Engineering* 77(4): 818 – 824.

Fitzpatrick J. 1998. Sludge processing by anaerobic digestion and superheated steam drying. *Water Research* 32(10): 2897 – 2902.

Fitzsimons, S.M., D.M. Mulvihill, and E.R. Morris. 2007. Denaturation and aggregation processes in thermal gelatin of whey proteins resolved by differential scanning calorimetry. *Food Hydrocolloids* 21(4): 638 – 644.

Gervais, M. 2008. Superheated steam processing system manual. Department of Biosystems Engineering, University of Manitoba, E1-369.

Graham, A.S., E. Jonas, A. Tanner, J. Avilo-Stagno, R.D. Bush, and A.V. Chaves. 2013. Effects of replacing rolled barley grain with wheat dry distillers' grains with solubles in Merino sheep rations. *Acta Agriculturae Scandinavia, Section A - Animal Science* 63(2): 101 – 110.

Hacihafizoglu, O., A. Cihan, K. Kahveci, and A. Lima. 2008. A liquid diffusion model for thin-layer drying of rough rice. *European Food Research and Technology* 226(4): 787 – 793.

Hashemi, G., D. Mowla, and M. Kazemeini. 2009. Moisture diffusivity and shrinkage of broad beans during bulk drying in an inert medium fluidized bed dryer assisted by dielectric heating. *Journal of Food Engineering* 92(1): 331 – 338.

Head, D., S. Cenkowski, S. Arntfield, and K. Henderson. 2011. Storage stability of oat groats processed commercially and with superheated steam. *LWT – Food Science and Technology* 44(1): 261 – 268.

Head, D.S., S. Cenkowski, S. Arntfield, and K. Henderson. 2010. Superheated steam processing of oat groats. *LWT – Food Science and Technology* 43(1): 690 – 694.

Holman, J. 2001. Heat Transfer. Boston, MA: McGraw – Hill. Tenth Ed.

Hyodo, T., and T. Yoshida. 1976. An experimental study of a closed circuit dryer. *Mechanical Engineering* 1: 17 – 21.

Ileleji, K.E., A. Garcia, A.R.P Kingsly, and C.L. Clementson. 2010. A comparison of standard methods to determine the moisture content of corn distillers dried grain with solubles. *Journal of AOAC International* 93(3): 825 – 832.

Incropera, F.B., and D.B. DeWitt. 1996. Fundamentals of heat and mass transfer (4 ed.). New York, NY: John Wiley & Sons, 226 – 230.

Iyota, H., N. Nishimura, T. Onuma, and T. Nomura. 2001. Simulation of superheated steam drying considering initial steam condensation. *Drying Technology* 19(1): 1425 – 1440.

Lane, D.M., D. Scott, M. Hebl, R. Guerra, D. Osherson, and H. Zimmer. Introduction to Statistics. Rice University.

Johnson, P., S. Cenkowski, and J. Paliwal. 2014. Analysis of the disintegration of distiller's spent grain compacts as affected by drying in superheated steam. *Drying Technology* 32(9): 1060 – 1070.

Johnson, P., S. Cenkowski, and J. Paliwal. 2013. Compaction and relaxation characteristics of single compacts produced from distiller's spent grain. *Journal of Food Engineering* 116(2): 260 – 266.

Karathanos, V.T., G. Villalobos, and G.D. Saravacos. 1990. Comparison of two methods of estimation of the effective moisture diffusivity from drying data. *Journal of Food Science* 55(1): 218 – 231.

Khurm, R.S. 2005. Steam Tables. S Chand & Co Ltd. Print.

Kim, S.S., and S.R. Bhowmik. 1995. Effective moisture diffusivity of plain yogurt undergoing microwave vacuum drying. *Journal of Food Engineering* 24(1): 137 – 148.

Kittiworrawatt, S., and S. Devhastin. 2009. Improvement of a mathematical model for low-pressure superheated steam drying of a biomaterial. *Chemical Engineering Science* 64(11): 2644 – 2650.

Lavasani, A.M., and T. Maarefdoost. 2014. Designing a low speed wind tunnel for investigating effects of blockage ratio on heat transfer of a non-circular tube. *International Journal of Mechanics, Aerospace, Industrial, and Mechatronics Engineering* 8(8): 1363 – 1366.

Li, Y.B., J. Seyed-Yagoobi, R.G. Moreira, and R. Yamsaengsung. 1999. Superheated steam impingement drying of tortilla chips. *Drying Technology: An International Journal* 17(1): 191 – 213.

Maroulis, Z.B., G.D. Saravacos, N.M. Panagiotou, and M.K. Krokida. 2001. Moisture diffusivity data compilation for foodstuffs: effect of material moisture content and temperature. *International Journal of Food Properties* 4(2): 225 – 237.

Mayor, L., and A.M. Sereno. 2004. Modeling shrinkage during convective drying of a food material: a review. *Journal of Food Engineering* 18(1): 373 – 386.

Moreira, G.R. 2001. Impingement drying of foods using hot air and superheated steam. *Journal of Food Engineering* 49(4): 291 – 295.

Mujumdar, A.S. 2000. Superheated steam drying – technology for the future. *Mujumdar's Practical Guide to Industrial Drying,* Devashatin, S., Ed. Brossard: Exergex. Canada: 115 – 138.

Mulet, A. 1994. Drying modeling and water diffusivity of carrots and potatoes. *Journal of Food Engineering* 22(1): 329 – 348.

Nomura, T., and T. Hyodo. 1985. Behavior of inversion point temperature and new applications of superheated vapour drying. *Drying 85'*: 804 – 809.

Nyachoti, C.M., J.D. House, B.A. Slominski, and I.R. Seddon. 2005. Energy and nutrient digestibilities in wheat dried distillers' grains with solubles fed to growing pigs. *Journal of the Science of Food and Agriculture* 85(15): 2581 – 2586.

OECD/Food and Agriculture Organization of the United Nations. 2014. OECD – FAO Agricultural Outlook 2014, OECD Publishing.

Pabis, S., D.S. Jayas, and S. Cenkowski. 1998. Grain Drying. New York, NY: John Wiley & Sons. Print.

Pirgozliev, S., N. Froese, and L. Paparcicova. 2009. Effect of CARAMBA 90 SL (metconazole) application on deoxynivalenol contamination in harvested grain of cereals. *Canadian Journal of Plant Pathology* 31(4): 495 – 496.

Potter, O.E., and C. Beeby. 1994. Scale-up of steam drying. *Drying Technology* 12(1): 179 – 215.

Pronyk, C., S. Cenkowski, and W.E. Muir. 2010. Drying kinetics of instant Asian noodles processed in superheated steam. *Drying Technology: An International Journal* 28(2): 304 – 314.

Pronyk, C., S. Cenkowski, W.E. Muir, and O.M. Lukow. 2008. Effects of superheated steam processing on the textural and physical properties of Asian noodles. *Drying Technology: An International Journal* 26(2): 192 – 203.

Pronyk, C., S. Cenkowski, and D. Abramson. 2006. Superheated steam reduction of deoxynivalenol in naturally contaminated wheat kernels. *Food Control* 17(10): 789 – 796.

Pronyk, C., S. Cenkowski, and W.E. Muir. 2004. Drying foodstuffs with superheated steam. *Drying Technology* 22(5): 899 – 916.

Rafiee, S., M. Sharifi, A. Keyhani, M. Omid, A. Jafari, S.S. Mohtasebi, and H. Mobli. 2010. Modeling effective moisture diffusivity of orange slice. *International Journal of Food Properties* 13(1): 32 – 40.

Rasco, B.A., G. Rubenthaler, M. Borhan, and F.M. Dong. 1990. Baking properties of bread and cookies incorporating distillers' or brewer's grain from wheat or barley. *Journal of Food Science* 55(2): 424 – 429.

Rovedo, C.O., and P.E. Viollaz. 2000. Drying of solids: the infinite slab condition. *Drying Technology* 18(1): 1007 – 1021.

Sano, A., Y. Senda, K. Oyama, R. Tanigawara, Y. Bando, M. Nakamura, Y. Sugimura, and M. Shibata. 2005. Drying characteristics in superheated steam drying at reduced pressure. *Drying Technology: An International Journal* 23(12): 2437 – 2447.

Shibata, H., J. Mada, and K. Funatsu. 1990. Prediction of drying rate curves on sintered spheres of glass beads in superheated steam under vacuum. *Industrial & Engineering Chemistry Research* 29(1): 614 – 617.

Shibata, H., and A.S. Mujumdar. 1994. Steam drying technologies: Japanese research & development. *Drying Technology* 6(12): 1485 – 1524.

Simal, S., C. Rosello, A. Berna, and A. Mulet. 1998. Drying of shrinking cylinder-shaped bodies. *Journal of Food Engineering* 37(1): 423 – 435.

Socolofsky, S.A., and G.H. Jirka. 2005. Special topics in mixing and transport processes in the environment (5 ed.). Texas A&M University: 1 – 19.

Sokolovskii, Y.I. 1998. Relationship between deformation-relaxation and heat-and-mass-transfer processes in the drying of capillary-porous bodies. *International Applied Mechanics* 34(7): 694 – 699.

Souraki, A.B., and D. Mowla. 2007. Axial and radial moisture diffusivity in cylindrical fresh green beans in a fluidized bed dryer with energy carrier: modeling with and without shrinkage. *Journal of Food Engineering* 109(1): 627 – 634.

Stroem, L.K., D.K. Desai, and A.F.A Hoadley. 2009. Superheated steam drying of brewer's spent grain in a rotary drum. *Advanced Powder Technology* 20(3): 240 – 244.

Taechapairoj, C., I. Dhuchakallaya, S. Soponronnarit, S. Wetchacama, and S. Prachayawarakorn. 2003. Superheated steam fluidised bed paddy drying. *Journal of Food Engineering* 58(1): 67 – 73.

Tang, H.Y. 2010. Design and functioning of low pressure superheated steam processing unit. Unpublished master's thesis, University of Manitoba, Department of Biosystems Engineering, Winnipeg, Canada.

Tang, Z., and S. Cenkowski. 2001. Equilibrium moisture content of spent grains in superheated steam under atmospheric pressure. *Transactions of the American Society of Agricultural Engineers* 22(5): 899 – 916.

Tatemoto, Y., Y. Mawatari, K. Sugita, K. Noda, and N. Komatsu. 2005. Drying characteristics of porous materials in a fluidized bed under reduced pressure. *Drying Technology* 23(6): 1257 – 1272.

Thuwapanichayanan, R., S. Prachayawarakorn, J. Kunwisawa, and S. Soponronnarit. 2011. Determination of effective moisture diffusivity and assessment of quality attributes of banana slices during drying. *LWT – Food Science and Technology* 44(1): 1502 – 1510.

Urbaniec, K., and J. Malczewski. 1997. Experimental investigations of beet pulp drying in superheated steam under pressure. *Drying Technology: An International Journal* 15(7): 2004 – 2013.

Woods, B., H. Husain, A.S. Mujumdar, and T. Kudra. 1995. Techno-economic assessment of potential superheated steam drying applications in Canada. *Drying Technology: An International Journal* 13(1): 505 – 506.

Wu, M., H. Xiao, W. Ren, J. Yin, B. Tan, G. Liu, L. Li, C.M. Nyachoti, X. Xiong, and G. Wu. 2014. Therapeutic effects of glutamic acid in piglets challenged with deoxynivalenol. *PLOS ONE* 9(7): 1 – 12.

Zielinska, M., and S. Cenkowski. 2012. Superheated steam drying characteristic and moisture diffusivity of distillers' wet grains and condensed distillers' solubles. *Journal of Food Engineering* 109(1): 627 – 634.